THERMAL FATIGUE ANALYSIS OF PRESSURE VESSELS WITH VARIOUS HEADS USING FEM

By

M. S. SURYANARAYANA

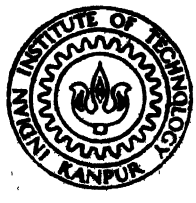

DEPARTMENT OF MECHANICAL ENGINEERING
INDIAN INSTITUTE OF TECHNOLOGY, KANPUR

MARCH, 1985

THERMAL FATIGUE ANALYSIS OF PRESSURE VESSELS WITH VARIOUS HEADS USING FEM

A Thesis Submitted
In Partial Fulfilment of the Requirements
for the Degreè of
MASTER OF TECHNOLOGY

By
M. S. SURYANARAYANA

to the

DEPARTMENT OF MECHANICAL ENGINEERING
INDIAN INSTITUTE OF TECHNOLOGY, KANPUR
MARCH, 1985

CERTIFICATE

This is to certify that the present work entitled, "THERMAL FATIGUE ANALYSIS OF PRESSURE VESSELS WITH VARIOUS HEADS USING FEM" by M.S. Suryanarayana has been carried out under my supervision and has not been submitted elsewhere for the award of a degree.

Bhupinder Pal Singh.

IIT Kanpur
March 1985

B.P. Singh
Assistant Professor
Mechanical Engineering Department
INDIAN INSTITUTE OF TECHNOLOGY, KANPUR

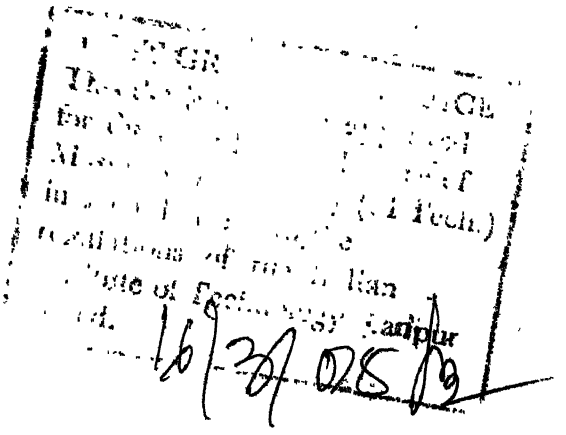

ACKNOWLEDGEMENTS

I express my sincere gratitude to my thesis supervisor, Dr. B.P. Singh, for his constant encouragement and excellent guidance throughout the span of this work.

I am thankful to my friends, K.G. Shastry, K. Subramanya for their help throughout this work. I am also thankful to my friend, V.V.S.N. Murthy for his excellent help during the development of computer program.

Also I thank H.K. Nathani for his excellent typing of this manuscript.

- M.S. Suryanarayana

IIT Kanpur
March 1985

CONTENTS

LIST OF TABLES

LIST OF FIGURES

ABSTRACT

In this work, thermal fatigue analysis of pressure vessels with hemispherical, elliptical, torispherical and toriconical heads has been studied using finite element method. Inside of the vessel is subjected to pressure and cylic temperature variation of heating, holding and cooling; and outside is insulated. Weight of the vessel has been considered and isoparametric eight noded quadrilateral ring elements have been used.

Stress variation is studied in all the vessels as function of heating/cooling rate and hold time. It is observed that maximum stress variation occurs in the skirt region near the head and is the dominant factor for the thermal fatigue life of the vessels with all heads. Vessel with hemispherical head is the best design, and others in this order are elliptical, torispherical and toriconical heads.

Finally the design changes are considered to reduce the stress variation in the skirt. One is to change the position of the skirt and other is to provide a portion of it a temperature variation as that of the inside of the vessel. The second method reduces the stress variation considerably.

CHAPTER I

INTRODUCTION

In recent years of research and development considerable attention has been focused on the design of pressure vessels because these are the means by which energy systems controlled, chemical and petroleum processes operated. Modern chemical processing plants and power generation industry demand the use of very high pressures and temperatures. Many chemical processing pressure vessels are subjected to a large number of temperature cycles, hence to stress cycles. Ultimately the vessel is liable to fail by thermal fatigue. Thus in such cases the designer is charged with the task of doing thermal fatigue analysis. This can only be done by a careful stress analysis of the entire vessel.

1.1 PREVIOUS WORK

Pressure vessels and its components are designed based on the standard codes like ASME, BS etc. However, the designer is often faced with complex loadings which are not covered by the codes. Thus certain designs fall beyond the scope of the code. One such loading is that of the inside surface of the vessel being subjected to cyclic temperature variation. This will induce transient thermal stresses which depend on the temperature attained and the thermal gradients caused. It is not possible to estimate the temperatures and the corresponding thermal stresses, as closed form relations are not

available. So a design of the vessel is completed on the basis of mechanical loads.

When once this design is completed, a detailed thermal stress analysis is needed when the vessel is subjected to thermal transients. In thermal fatigue problems, the designer is interested in knowing what is the critical section, where the stresses are going to be maximum. Also for calculating the allowable number of thermal cycles, knowledge of maximum alternating stress or strain amplitude is essential.

Stress analysis of pressure vessels can be performed by the following methods:

1. Analytical Methods
2. Experimental Methods which include
   a. Strain gauge measurement
   b. Photoelastic method
   c. Brittle coating method
3. Numerical Techniques.

Analytical methods require a general solution of the equilibrium equations. But sometimes the problem becomes too complex and beyond analytical solution. Then one has to resolve to experimental methods. But the experimental methods pose a lot of difficulties in the fabrication of the model and creating the required type of loading. This needs a lot of skill and is highly costly in time and money.

Thus in recent times, Numerical Techniques such as finite element method has been used for the stress analysis. In FEM, the continuum is divided into a finite number of elements. A solution for the displacements is assumed initially in the form of a polynomial without giving any consideration to the boundary

conditions of the problem. Now using either variational principles or weighted residual methods, typical finite element equations between stiffness, displacements and load matrices are formed. These elemental equations are suitably assembled and global equations are formed. Then by applying the boundary conditions, the system of equations are solved for the displacements and later strains and stresses are found at various points. In this way a general FEM program can handle a variety of problems of Solid Mechanics, Heat Transfer and Fluid Mechanics. The development of modern computers with tremendous speeds of calculation made FEM to emerge as a powerful numerical technique in the field of stress analysis. The results from the FEM are in excellent agreement with theoretical exact solutions available for some problems.

Langer [1] reported that since most pressure vessels are subjected to limited number of pressure and temperature cycles during the life time, considerable design effort could be saved by defining the conditions which do or do not require a fatigue evaluation. The author in his study concluded that a fatigue evaluation is needed if during normal operation,

1. Pressure fluctuates through a range exceeding twenty-five percent of the design pressure, or
2. The temperature difference between any two adjacent points in the vessel changes by more than 22°C (40°F).

This makes it possible to eliminate a great deal of detailed calculations for vessels that are subjected to pressure and temperature cycles of moderate severity.

Pickett and Grigory [2] reviewed the fatigue evaluation procedures and the fracture mechanics approach to fatigue life analysis. They made important remarks on crack initiation, crack propagation and about the fatigue test specimens. They mentioned that specimens loaded in bending are better compared with axial or push pull type specimens. They concluded that the surface strains at the test section on bending specimens shake down to stable values after a few cycles and can be measured easily.

Most studies of low cycle fatigue behaviour have been concerned with evaluating the effects of cyclic frequency and holding time at peak strain or stress.

Conway, Berling and Stenz [3] did an experimental work using servocontrolled, hydraulically actuated fatigue machines which subjected inductively heated specimens to a push pull type of loading. They developed a diametral strain extensometer and the signal from this device and from the load cell in series with the specimen was fed to a specially designed computer network to provide for axial strain control.

They reported that hold period at peak stress or peak strain leads to reduction in the cyclic fatigue life. They also reported that the time to fracture is proportional to the length of the hold period. This effect is just opposite to the number of cycles to fracture. As the length of the hold period increases, number of cycles to cause failure decreases.

Saraph, Kushwaha and Kakodkar [4] worked on transient thermal stress analysis of pressure vessels using finite element

method. They studied the problem of thermal shock, one of the most severe loadings experienced by light water cooled reactor vessel, when it is subjected to emergency cooling. They modelled the vessel as an axisymmetric geometry with eight noded isoparametric finite elements. The transient temperatures were calculated by Crank-Nicholson's scheme. Detailed temperature and stress plots were given. The authors had taken a cylindrical vessel with a hemispherical head which is the most common one in nuclear industry.

1.2 PRESENT WORK

In design of vessels subjected to mechanical (pressure) and thermal loads, both should be given proper importance. Because, the principles upon which thermal stresses can be mitigated are many times different to those involved in designing for mechanical load. For example, making of sections of large thickness can reduce the operating stresses for mechanical loads. But this approach may increase thermal stresses, as high thermal gradients are set up in relatively thick vessel walls.

In chemical and petrochemical industries, pressure vessels with hemispherical, elliptical, torispherical and toriconical heads are quite common. Hence in the present work, thermal fatigue analysis of pressure vessels with four types of heads mentioned above has been studied using the FEM. Thermal stress calculations need prior knowledge of temperature distribution. Both temperatures and thermal stresses have been determined by the finite element method. Although

still it is more popular to use finite difference method for temperature calculations but here FEM has been used. As FEM is very straight forward method and implementation of boundary conditions is an extremely simple affair. In addition use of FEM for temperature and thermal stress calculations reduces the overall data preparation as same mesh is used for both.

It is known that higher order elements give the same accuracy with fewer number of elements. This also requires much less data preparation. In addition pressure vessels have many curved surfaces. So the isoparametric eight noded quadrilateral ring elements have been used for temperature and thermal stress calculations.

In the present work, pressure vessels are supported by skirts. Insides of the vessels are subjected to cyclic temperature variation of heating, holding and cooling and outsides are insulated.

Allowable number of cycles as function of heating/cooling rate and hold time are calculated. It is found that maximum stress variation occurs in the skirt near the head and is the controlling factor for the life of the vessels. So design modifications are considered to reduce these stress variations in the skirt and thus improve the life of the vessel.

CHAPTER II

FORMULATION

Finite element method is used for the thermal fatigue analysis of pressure vessels in this work. Calculation of the thermal stresses requires the temperature distribution. First the method to determine the temperature distribution is given and then the method to determine thermal stresses is given. Details of these methods are available in the text [6] but are included here to make the thesis self-contained.

As the aim of the thesis is to study the thermal fatigue life of pressure vessels with various heads, design of vessels with elliptical, torispherical and toriconical heads is also given in this chapter.

2.1 TRANSIENT TEMPERATURE CALCULATION

Pressure vessels under consideration are axisymmetric bodies subjected to axisymmetric temperature distribution on the inside and insulated on the outside. Thus the temperature distribution is independent of θ coordinate. Therefore, the governing differential equation for the temperature T is [7]

$$\frac{\partial^2 T}{\partial r^2} + \frac{1}{r}\frac{\partial T}{\partial r} + \frac{\partial^2 T}{\partial z^2} = \frac{1}{a}\frac{\partial T}{\partial t} \qquad (1)$$

where a is the thermal diffusivity.

For this problem finite elements become ring elements. To take care of curved boundaries, isoparametric eight noded quadrilateral elements are taken as shown in Fig. 1.

Temperature distribution over the element is taken as

$$T^{(e)} = [N]\{T\}^{(ne)} \tag{2}$$

where $[N]$ are the interpolating functions and $\{T\}^{(ne)}$ are the temperatures at the nodes.

Substitution of Eqn. (2) in Eqn. (1) gives the residue of the element. This residue is minimised by the Galerkin method and finally one gets

$$[C]^{(e)}\{\dot{T}\}^{(ne)} + [K]^{(e)}\{T\}^{(ne)} = \{q\}^{(ne)} \tag{3}$$

where

$$[C]^{(e)} = \iint \frac{1}{a} r \{N\}[N]\, dr\, dz$$

$$[K]^{(e)} = \iint r(\{N,r\}[N,r] + \{N,z\}[N,z])\, dr\, dz$$

and

$$\{q\}^{(ne)} = \oint \{N\}\left(\frac{-q}{k}\right) r\, dB \tag{4}$$

$[C]^{(e)}$ is the thermal capacitance matrix, $[K]^{(e)}$ is the thermal stiffness matrix and $\{q\}^{(ne)}$ is the boundary heat flux matrix.

2.2 THERMAL STRESSES, FEM FORMULATION

The potential to be minimised is

$$I = \tfrac{1}{2}\int \sigma\epsilon\, dV - \int F_i u_i dV - \int S_i u_i ds \tag{5}$$

Here the first term represents the strain energy, the second term represents the work done by body forces and the third term represents the work done by surface forces.

The pressure vessels under consideration are axisymmetric bodies subjected to axisymmetric pressure and temperature loadings.

Thus the displacements, strains and stresses are independent of θ coordinate. Thus for this problem also finite elements become ring elements as for temperature distribution problem. Same isoparametric eight noded quadrilateral elements shown in Fig. 1 are taken for this problem, but here each node will have the degrees of freedom u and v.

The displacements over the finite element are taken as

$$\begin{Bmatrix} u \\ v \end{Bmatrix}^{(e)} = \begin{bmatrix} N_1 & 0 & N_2 & 0 & \cdots & \cdots \\ 0 & N_1 & 0 & N_2 & \cdots & \cdots \end{bmatrix} \begin{Bmatrix} u_1 \\ v_1 \\ u_2 \\ v_2 \\ \vdots \end{Bmatrix}$$

$$\{u\}^{(e)} = [N(r,z)]\,\{u\}^{(ne)} \tag{6}$$

Here u is the displacement in the r-direction and v is the displacement in the z-direction.

The strain matrix for this axisymmetric problem is, [6]

$$\{\epsilon\} = \begin{Bmatrix} \epsilon_r \\ \epsilon_\theta \\ \epsilon_z \\ \gamma_{rz} \end{Bmatrix} = \begin{Bmatrix} \frac{\partial u}{\partial r} \\ \frac{u}{r} \\ \frac{\partial v}{\partial z} \\ \frac{\partial u}{\partial z} + \frac{\partial v}{\partial r} \end{Bmatrix} \tag{7}$$

Using Eqn. (6), the strain matrix $\{\epsilon\}$, Eqn. (7) becomes

$$= [B]\,\{u\}^{(ne)} = [B]_i \begin{Bmatrix} u \\ v \end{Bmatrix}_i \tag{8}$$

where

$$[B]_i = \begin{bmatrix} \frac{\partial N_i}{\partial r} & 0 \\ \frac{1}{r} N_i & 0 \\ 0 & \frac{\partial N_i}{\partial z} \\ \frac{\partial N_i}{\partial z} & \frac{\partial N_i}{\partial r} \end{bmatrix} \tag{9}$$

The stress-strain matrices are related to each other as,[6],

$$\{\sigma\} = [D](\{\epsilon\} - \{\epsilon_0\}) \tag{10}$$

where [D] is the elasticity matrix and $\{\epsilon_0\}$ is the thermal strain matrix, and these are,

$$[D] = \frac{E(1-\nu)}{(1+\nu)(1-2\nu)} \begin{bmatrix} 1 & \frac{\nu}{1-\nu} & \frac{\nu}{1-\nu} & 0 \\ & 1 & \frac{\nu}{1-\nu} & 0 \\ \text{sym} & & 1 & 0 \\ & & & \frac{1-2\nu}{2(1-\nu)} \end{bmatrix} \tag{11}$$

$$\{\epsilon_0\} = \begin{Bmatrix} \alpha T \\ \alpha T \\ \alpha T \\ 0 \end{Bmatrix} \tag{12}$$

Here α is the coefficient of linear thermal expansion and T is the temperature rise.

Using Eqns. (6), (8) and (10), Eqn. (5) becomes,

$$I = \tfrac{1}{2}\{u\}^{(ne)}(2\pi)\iint[B]^T[D][B]rdrdz\ \{u\}^{(ne)} - \{u\}^{(ne)}\ 2\pi\iint[B]^T[D]\{\epsilon_0\}rdrdz - \{u\}^{(ne)}\ 2\pi\iint[N]^T prds - \{u\}^{(ne)}\ 2\pi\iint[N]^T Frdrdz \quad (13)$$

By applying the Raylcigh Ritz method, one gets,

$$[K]^{(e)}\ \{u\}^{(ne)} = \{F_0\}^{(ne)} + \{F_s\}^{(ne)} + \{F_B\}^{(ne)} \quad (14)$$

where

$$[K]^{(e)} = 2\pi\iint[B]^T[D][B]rdrdz$$

$$\{F_0\}^{(ne)} = 2\pi\iint[B]^T[D]\{\epsilon_0\}rdrdz$$

$$\{F_s\}^{(ne)} = 2\pi\iint[N]^T prdB$$

$$\{F_B\}^{(ne)} = 2\pi\iint[N]^T Frdrdz \quad (15)$$

Here $[K]^{(e)}$ is the stiffness matrix, $\{F_0\}^{(ne)}$ is the thermal load matrix, $\{F_s\}^{(ne)}$ consistent surface load matrix and $\{F_B\}^{(ne)}$ is body force matrix.

In this present problem surface loads are the internal pressures acting normal to the surface as shown in Fig. 19. The consistent surface load matrix is,

$$\{F\}^{(ne)} = 2\pi\int[N]^T\begin{Bmatrix}p_r\\p_z\end{Bmatrix}rdB \quad (16)$$

If the pressure is acting along the edge $\eta = +1$, then

$$p_r = p\frac{dz}{dB} \quad \text{and} \quad p_z = -p\frac{dr}{dB}$$

$$\text{or } p_r\,dB = pdz = p\frac{\partial z}{\partial \xi}d\xi \quad \text{and} \quad p_z dB = -pdr = -p\frac{\partial r}{\partial \xi}d\xi \quad (17)$$

Substituting Eqn. (17) in Eqn. (16), one gets,

$$\{F\}^{(ne)} = 2\pi \int_{-1}^{1} p[N]^T \begin{Bmatrix} \frac{\partial z}{\partial \xi} \\ -\frac{\partial r}{\partial \xi} \end{Bmatrix} r \, d\xi \qquad (18)$$

Similar expressions for other edges is $\eta = -1$ and $\xi = \pm 1$ can be written. Value of this integral is determined by Gauss Legendre numerical integration.

Body force in the present problem is gravitational force. Thus the body force matrix becomes,

$$\{F_B\}^{(ne)} = 2\pi\rho \iint [N]^T \begin{Bmatrix} 0 \\ g_z \end{Bmatrix} r dr dz \qquad (19)$$

2.3 METHOD OF SOLUTION

2.3.1 Determination of Matrices

All the matrices developed in Sections 2.1 and 2.2 are evaluated by Gauss Legendre numerical integration scheme. In this scheme the quadrilateral is first transformed into a square of side 2. Then the function inside the integral is evaluated at each Gauss point, and multiplied by the corresponding weight. Sum of these products give the value of the integrals and thus the matrices. 2x2 point integration has been used in this work.

Determination of thermal load matrix $\{F_0\}^{(ne)}$ of Eqn. (15) needs some comments. In this matrix, one needs the temperature rise T. Reference [6] suggests that this be taken as average temperature rise of the nodes of the element. This does not seem to be an accurate method for evaluation of this matrix. It is more accurate to determine the temperature rise at every Gauss points and use it while doing the numerical integration.

2.3.2 Temperature Determination

Eqn. (3) are first order simultaneous differential equations. They are solved here by finite difference method. Thus $\dot{T}_i$ at any time at i^{th} node can be expressed as,

$$\dot{T} = \frac{T_i^{p+1} - T_i^p}{\Delta t}$$

and

$$T_i = \theta\, T_i^{p+1} + (1-\theta) T_i^p \qquad (20)$$

where p refers to previous time step and p + 1 refers to the current time.

Using Eqn. (20), Eqns (3) become,

$$\left(\frac{1}{t}[C]^{(e)} + \theta[K]^{(e)}\right)\{T\}^{(ne)}\Big|^{p+1} = \left(\frac{1}{t}[C]^{(e)} - (1-\theta)[K]^{(e)}\right)\{T\}^{(ne)}\Big|^{p} + \{q\}^{(ne)}\Big|^{p} \qquad (21)$$

or

$$[E]^{(e)}\{T\}^{(ne)}\Big|^{p+1} = [L]^{(e)}\{T\}^{(ne)}\Big|^{p} + \{q\}^{(ne)}\Big|^{p} \qquad (22)$$

These matrices $[E]$ and $[L]$ can be evaluated once θ and Δt are fixed. These equations are assembled for the whole domain and boundary conditions are applied. The assembled equations are simultaneous algebraic equation and are solved by Gauss elimination method. This way temperatures at all the time steps of the cycle are determined.

Value of θ was taken as 1.0 in this work and is discussed in Chapter III.

2.3.3 Thermal Stress Determination

Finite element eqns. (14) are assembled in the usual way and boundary conditions applied. These are simultaneous algebraic equations and are solved by Gaussian elimination for displacements. Stresses are determined using Eqn. (10).

2.4 DESIGN OF VARIOUS PRESSURE VESSEL HEADS

A design of the pressure vessel with hemispherical heads done by Bharat Heavy Plate & Vessels has been available with Department of Mechanical Engineering, Indian Institute of Technology, Kanpur. Elliptical, torispherical and toriconical heads are designed for the vessel using ASME code given by Chuse & Eber [11].

Design details available for vessel with hemispherical heads

Design pressure	28 MPa
Working pressure	26 MPa
Code followed	ASME 1980-81,SEC VIII
Material of the vessel	SA 336 Gr F11
Design stress intensity of the material	155 MPa
Yield strength	275 MPa
Ultimate tensile strength	480 MPa
Thermal diffusivity	9.4936×10^{-6} $m^2/sec.$
Coefficient of linear expansion	12.474×10^{-6}
Density of the material	7860 kg/m^3

The Fig. 2 gives the other design details of this vessel with hemispherical head.. The thickness of the hemispherical

head has been calculated by the following relation [11]

$$t = \frac{PR}{2SE - 0.2P} \tag{23}$$

where P = internal pressure

R = inside radius of head as shown in Fig. 2

S = allowable stress

E = joint efficiency.

Elliptical head: Thickness of the elliptical head is given by [11]

$$t = \frac{PD}{2SE - 0.2P} \tag{24}$$

where D is the head skirt diameter. This head has been designed for a major axis to minor axis ratio of 2:1. Thickness comes out to be 140mm. Other details are shown in Fig. 3.

Torispherical head: The thickness of the torispherical head is given by [11]

$$t = \frac{0.885\ PL}{SE - 0.1P} \tag{25}$$

where L is the inside crown radius. L has been taken 974mm in this design. With this, head thickness comes out to 155mm. Knuckle radius has been taken as 6% of the inside crown radius as required by ASME code [11]. Other details are given in Fig. 4.

Toriconical head: The thickness of the toriconical head is given by [11]

$$t = \frac{PD_1}{2\cos\alpha\,(SE-0.6P)} \tag{26}$$

where D_1 is the inside cone diameter at the point of tangency to the knuckle, α is one half of the apex angle. In this

design D_1 has been taken as 1435mm and α as 50°. Inside knuckle radius has been taken as 6% of the outside diameter of head skirt. Other details are given in Fig. 5.

CHAPTER III

RESULTS and DISCUSSION

As already mentioned, finite element method has been used for the study of thermal fatigue life of pressure vessels with different types of heads. The stress states in various heads have been studied. The effect of rate of change of temperature and hold period on the thermal fatigue life of the pressure vessels has also been studied.

3.1 CHECKING THE VALIDITY OF THE PROGRAM DEVELOPED

To check the validity of the finite element program developed, a test problem given in [5] was used. Also the problem of thick sphere under internal pressure and steady state temperature given in [6] was used. A good agreement of the results with the available solutions was observed.

3.2 TRANSIENT TEMPERATURE DISTRIBUTION

For transient temperature calculations, both explicit ($\theta = 0$) and implicit ($\theta \neq 0$) were tried with, to find the value of θ which will give minimum or no oscillations of temperatures. Generally it is accepted that θ greater than 1/2 will give less oscillations [6]. Values of θ as 0, $\frac{1}{2}$, $\frac{2}{3}$ (Galerkin's scheme) and 1 (fully implicit) were tried. It was found that fully implicit scheme of $\theta = 1$ gave almost zero oscillations. So in this work this scheme has been used through out.

3.3 STRESS COMPUTATION AND ASSESSMENT OF FATIGUE LIFE

After calculating the temperatures in the vessel at various time steps of the thermal cycle, stresses were determined. The temperature and stresses in the vessel were determined using 2 x 2 point integration. It was observed that the stresses in the vessel reached an extreme at the end of the heating portion of the cycle and reached another extreme at the end of the cooling portion of the cycle. This was found to be true for all types of thermal cycles i.e., with or without any hold period. As only maximum alterating stress amplitude was needed for the fatigue life evaluation, stresses were calculated only at these two points of the thermal cycle i.e., at the end of heating and cooling portions. In this way, a lot of computer time was saved by avoiding the stress calculations at every instant of the thermal cycle.

Further it was observed that the principal stress directions at the above extreme points of thermal cycle were different. So to find the stress amplitude, the method given by ASME code [12] was used, which is as follow: The stresses σ_r, σ_θ, σ_z and τ_{rz} at the two extreme points are calculated and subtracted. These stress differences are denoted by σ_r', σ_θ', σ_z' and τ_{rz}'. The principal stresses corresponding to these stress differences are denoted by σ_1', σ_2', σ_3' and their differences as $\sigma_1' - \sigma_2'$, $\sigma_2' - \sigma_3'$ and $\sigma_3' - \sigma_1'$. Half of the maximum difference gives the maximum stress amplitude. The

allowable number of fatigue cycles are determined using the design fatigue curve given in ASME code [12].

3.4 STRESS STATE IN VARIOUS VESSELS

All vessels are subjected to an internal pressure of 26 MPa. Insides of the vessels are subjected to temperature cycles, typical one is shown in the Fig. 6, and outsides are insulated. Temperatures vary from 5°C to 245°C on the inside. Two rates of heating/cooling of 1°C/m and 1.5°C/m are studied. For each heating/cooling rate five hold periods of 0,1,2,3 and 4 hours are considered. The thermal cycle with heating/cooling rate of 1.0°C/min and 2 hours of hold period is called here as a typical cycle.

3.4.1 Stress Distribution Due to Mechanical Loads

Maximum principal stress in upper head, cylindrical portion and in lower head is shown in Table 2.

Table 2: Maximum Principal Stress, MPa

Vessel with	Upper Head	Lower Head	Cylindrical
Hemispherical Head	152	173	136
Elliptical Head	184	182	142
Torispherical Head	175	189	141
Toriconical Head	117	126	141

It is seen that the principal stresses are more in the lower head than in the upper head except in the vessel with elliptical heads. These stresses are essentially same in the cylindrical portion. Principal stress in upper head is maximum in the elliptical head and minimum in toriconical head. Principal stress in the lower head is maximum in the torispherical head and minimum in toriconical head. It is also observed that this maximum principal stress occured on the inner side for all the heads.

Maximum principal stress across AA in the upper heads is shown in Fig. 7. It is seen that it essentially remains constant across the thickness in hemispherical head, and fall very sharply in the other heads.

3.4.2 Temperature Distribution

Temperature distribution in the vessel with spherical heads at the end of heating is shown in Fig. 8 and at the end of cooling in Fig. 9. These are for a typical thermal cycle in the similar way temperatures are calculated for other vessels and subsequently used for stress calculations.

3.4.3 Stress Distribution Due to Mechanical and Thermal Loading

Maximum principal stresses in upper head, cylindrical portion, lower head and skirt at the end of heating and cooling are given in Table 3. These are for typical thermal cycle.

It is observed that generally maximum principal stress occured in lower heads both at the end of heating and cooling. Also it is observed that maximum principal stress occured at

the end of cooling in all sections of the vessles except in the skirt. It is seen that the maximum principal stress in the cylindrical portions of all the vessels at the end of heating remained more or less same. The same is observed at the end of cooling. It may be noted that maximum values at the end of heating and cooling many a times do not occur at the same point.

Maximum principal stress across AA in the upper heads is shown in Figs. 10 and 11. It is observed that maximum principal stress in all the heads occured at the inside surface and falls sharply across the thickness.

Maximum principal stress across the cylindrical portion BB of the vessel with spherical head is shown in Fig. 12.

In Figs. 13 and 14 the variation of maximum principal stress in various heads in a typical thermal cycle is shown. These can be referred to as typical stress cycles produced in various heads and are drawn at a point in an element where stress amplitude is observed to be maximum. It is observed from these figures that the hemispherical head is having the least stress amplitude. It is observed that the stress amplitude is increasing in the order of elliptical, torispherical and toriconical heads. In Fig. 15 the variation of maximum principal stress in a typical thermal cycle in the cylindrical portion of the vessel with hemispherical heads is shown.

It is observed from thse graphs that during the heating portion of thc cycle, the thermal stresses in the element considered are compressive and during the cooling portion they change to tensile stresses.

3.5 THERMAL FATIGUE LIFE

In this study, two heating/cooling rates of 1.0 and 1.5°C/m with five different hold periods as detailed in Table 1 are considered. Thermal stresses and maximum stress amplitudes are calculated as explained in Section 3.3.

Maximum stress amplitudes for these thermal cycles for vessels with different heads are given in Tables 4 and 5 for 1 and 1.5°C/m respectively. It is seen that these amplitudes hardly change in the upper head and cylindrical portions, slightly change in the lower heads and considerably change in the skirt regions. for all the vessels. Also it is seen that these amplitudes are more in the lower heads than those in the upper heads due to the proximity of skirt near the lower heads. It is observed that maximum stress amplitude always occurs in the skirt region near the vessel. Values of these amplitudes are shown in Fig. 16 for various vessels for different hold periods. As expected the maximum stress amplitudes increase with increase in hold period and heating/cooling rate. It is seen that these amplitudes increase in the order of hemispherical, elliptical, torispherical and toriconical head vessels.

Fatigue life of various vessels i.e., allowable number of fatigue cycles is calculated using the design fatigue curve given in ASME code [12]. Fatigue lives of various vessels for different heating/cooling rates and hold periods are shown in Table 6. For heating/cooling rate of 1°C/m these values are also given in Fig. 17 as functions of total cycle time. For heating/cooling rate of 1 and 1.5°C/m these values are given in Fig. 18 as functions of hold period. For vessels with hemispherical heads, with heating/cooling rate of 1.0°C/min, the fatigue life decreased by 23% from a no hold period to a hold period of four hours. For the same conditions mentioned above, the vessels with elliptical, torispherical and toriconical heads showed a decrease of 28%, 34% and 36% respectively.

With a heating/cooling rate of 1.5°C/min, a change in hold period from zero to four hours, vessels with hemispherical, elliptical, torispherical and toriconical heads show a decrease in fatigue l ife of 23%, 29%, 34% and 46% respectively.

For a hold period of 2 hours, change of heating/cooling rate from 1.0 to 1.5°C/m vessels with hemispherical, elliptical, torispherical and toriconical heads show a decrease in the fatigue life by 50%, 50%, 26%, 14% respectively.

3.6 METHODS TO REDUCE THE STRESS AMPLITUDE IN THE SKIRT REGION

Throughout the analysis, it is observed that high stress amplitudes are developed in the skirt region adjacent to the

head. The existing design of the skirt caused large thermal gradients at the skirt vessel junction, thereby producing high stress amplitudes. Thus in the entire analysis the skirt is found to be the predominant factor in reducing the fatigue life of the vessel. Because of the skirt, higher stress amplitudes are produced in the bottom head also. So efforts are made to reduce the stress amplitude in the skirt, thereby increasing the fatigue life of the vessel. The two methods which successfully reduced the stress amplitude in the skirt are as below:

1. Changing the position of the skirt.
2. Providing a suitable temperature distribution in the skirt.

In the existing designs the skirt is attached at the head-cylinder junctions. In the new design, the position of the skirt is changed and attached only to the head region as shown in the Fig. 2. This change in design is studied in the vessel with hemispherical head only. For the no hold time thermal cycle with 1.0°C/min heating/cooling rate, the new design reduces the stress amplitude by about 10%. But even this 10% decrease in stress amplitude does not increase the fatigue life much. So a second method mentioned above has been tried with.

In this second approach, a favourable temperature distribution is provided at the skirt to decrease the existing high thermal gradients. Hence one fourth length of skirt

adjacent to the head has been subjected to the same thermal cycle as that of the inside of the pressure vessel. The required temperature variation with the desired rate of change of temperature may be brought by using electric heating coils around that skirt. This change considerably decreases the thermal gradients at the skirt vessel junction and hence the stress amplitude. For a heating/cooling rate of 1°C/m, maximum stress amplitudes in upper head, cylinder, lower head and skirt of various vessels are shown in Table 7. Results for these cases without skirt heating are also given in this Table. Maximum stress amplitudes decrease considerably in lower heads and skirts. Decrease in skirts is almost dramatic. For vessels with hemispherical, elliptical and toriconical heads skirt is no more the design criterion. Fatigue life for vessels with hemispherical and elliptical heads become infinite. Fatigue life for vessels with torispherical and toriconical head increase by 50% and 45% respectively. It is felt that fatigue life of torispherical head can be further improved by shifting the skirt and modifying the heating rate of the skirt.

CHAPTER IV

CONCLUSIONS

In this thesis thermal fatigue life of vessels with four types of heads namely hemispherical, elliptical, torispherical and tericonical heads have been studied. Insides of the vessels are subjected to heating, holding and cooling and outsides insulated.

It is observed that maximum stress variation occurs in the skirt region near the head and is the dominant factor for the thermal fatigue life of the vessels with all heads. Of the four types of vessels studied, the vessel with hemispherical heads has the highest thermal fatigue life. The thermal fatigue life of the vessels decreases in the order of elliptical, torispherical and toriconical heads.

If stress variation only in the heads is considered, it is again observed that hemispherical heads have the minimum variation.

It is seen that thermal fatigue life decreases with increase in heating/cooling rate and hold time as expected. The decrease is least in the vessel with hemispherical heads. The thermal fatigue life decreases in the order of elliptical, torispherical and toriconical heads.

Two methods were studied to reduce the variation of thermal stresses in the skirt near the head. One was changing the position of the skirt and other was to subject

the one fourth of the skirt adjacent to the head to the same temperature variation as that of the inside of the vessel. The first method does not reduce stress variation much. The second method reduces variation considerably. This reduction is dramatic in case of spherical and elliptical heads.

REFERENCES

1. Langer, B.F., "Design of Pressure Vessels for Low Cycle Fatigue," Transactions of ASME, Journal of Basic Engineering, Vol. 84, September 1962, pp. 389-402.
2. Pickett, A.G., and Grigory, S.G., "Prediction of the Low Cycle Fatigue," Transactions of ASME, Journal of Basic Engineering, Vol. 89, December 1967, pp. 858-870.
3. Conway, J.B., Berling, J.T., and Stenz, R.H., "Correlating the Effects of Hold Time and Strain Rate on Low-Cycle Fatigue Behaviour," Proceedings of the International Conference held at Berkeley Castle, England, September 22nd to 26th, 1969, pp. 89-107.
4. Saraph, H., Kushwaha, H.S., and Kakodkar, A., "Transient Thermal Stress Analysis by Finite Element Method," Conference on Pressure Vessel Technology, 1980, Organized by R&D Establishment, Pune, BARC, Bombay and Indian Vacuum Society, Bombay.
5. Smith, I.M., "Programming the Finite Element Method with Application to Geotechniques", John Wiley & Sons, New York, 1982.
6. Zienkiewicz, O.C.,"The Finite Element Method," Tata McGraw-Hill Publishing Company Limited, New Delhi, 1979.
7. Eckert, E.R.G., and Robert M. Drake, Jr., "Heat and Mass Transfer," Tata McGraw-Hill Publishing Company Limited, New Delhi, 1979.

8. John F. Harvey, "Theory and Design of Modern Pressure Vessels", Van Nostrand Reinhold Company, New York, 1974.
9. Nichols, R.W., "Pressure Vessel Engineering Technology," Applied Science Publishers Ltd., London, 1971.
10. Lloyd E., Brownell, and Edwin H. Young, "Process Equipment Design," Wiley Eastern Limited, New Delhi, 1983.
11. Robert Chuse, Stephen, M.,Eber, P.E., "Pressure Vessels - The ASME Code Simplified," McGraw-Hill Book Company, 1984.
12. "ASME Boiler and Pressure Vessel Code,", 1980.

Table 1: Thermal Cycles Studied

Sl No	Temperature Change, °C	Rate of Change of Temperature, °C/min.	Time for heating/ cooling, minutes	Hold Periods, minutes				
				Case 1	Case 2	Case 3	Case 4	Case 5
1	5 to 245	1.0	240	0	60	120	180	240
2	5 to 245	1.5	160	0	60	120	180	240

Table 3: Maximum Principal Stress, MPa

Vessel with	Upper Head		Cylinder		Lower Head		Skirt	
	End of heating	End of cooling	End of heating	End of cooling	End of heating	End of cooling	End of heating	End of cooling
Hemispherical Head	161	174	143	178	165	201	150	91
Elliptical Head	173	216	152	182	174	214	-106	74
Torispherical Head	129	220	150	180	151	229	-251	-74

Table 4: Maximum Stress Amplitudes (MPa) in Various Pressure Vessels with heating/cooling rate of 1°C/m.

Sl No	Section	Hold Period Min.	Hemispherical		Elliptical		Torispherical		Toriconical	
			S_a	El. No	S_a	El.No	S_a	El.No	S_a	El.No
1	Upper head	0	25.5	9	33.6	9	48.7	1	92.6	3
		60	25.5	9	33.6	9	48.7	1	93.1	3
		120	25.5	9	33.6	9	48.7	1	93.3	3
		180	25.5	9	33.6	9	48.7	1	93.3	3
		240	25.5	9	33.6	9	48.7	1	93.3	3
2	Cylin-der	0	40.4	19	42.4	31	46.0	31	74.6	31
		60	40.4	19	42.6	31	46.1	31	75.2	31
		120	40.4	19	42.7	31	46.2	31	75.6	31
		180	40.4	19	42.8	31	46.3	31	75.8	31
		240	40.4	19	42.8	31	46.4	31	76.0	31
3	Lower head	0	40.4	38	70.0	36	61.1	36	106.3	41
		60	41.4	38	71.5	36	62.4	36	107.4	41
		120	42.2	38	72.6	36	63.3	36	108.2	41
		180	42.9	38	73.5	36	64.0	36	108.6	41
		240	43.5	38	74.2	36	64.7	36	109.0	41
4	Skirt	0	107.4	47	131.9	47	132.8	47	153.5	48
		60	109.8	47	135.3	47	137.7	47	159.9	48
		120	111.8	47	137.9	47	141.5	47	164.9	48
		180	113.4	47	140.0	47	144.6	47	168.9	48
		240	114.8	47	141.8	47	147.2	47	172.1	48

Table 5: Maximum Stress Amplitudes (MPa) in Various Vessel Heads with a heating and cooling rate of 1.5°C/min.

Sl No	Section	Hold Period Min.	Hemispherical		Elliptical		Torispherical		Toriconical	
			S_a	El. No	S_a	El.No	S_a	El.No	S_a	El.No
1	Upper head	0	38.1	9	50.2	9	72.5	1	131.4	3
		60	38.1	9	50.3	9	72.7	1	133.8	3
		120	38.1	9	50.3	9	72.7	1	134.5	3
		180	38.1	9	50.3	9	72.7	1	134.8	3
		240	38.1	9	50.3	9	72.7	1	134.9	3
2	Cylinder	0	60.3	23	61.8	31	67.0	31	103.9	31
		60	60.4	23	62.1	31	67.3	31	105.7	31
		120	60.4	19	62.3	31	67.5	31	106.5	31
		180	60.4	19	62.4	31	67.6	31	107.0	31
		240	60.4	19	62.5	31	67.7	31	107.4	31
3	Lower Head	0	52.7	35	86.7	36	76.8	36	144.1	41
		60	53.3	35	89.3	36	79.0	36	147.6	41
		120	53.7	35	91.1	36	80.5	36	149.3	41
		180	53.9	35	92.5	36	81.6	36	150.2	41
		240	54.2	35	93.6	36	82.4	36	150.8	41
4	Skirt	0	129.0	47	155.1	47	145.4	47	152.8	48
		60	133.4	47	161.2	47	152.3	47	163.9	48
		120	136.5	47	165.5	47	157.0	47	172.1	48
		180	138.9	47	168.7	47	160.0	47	178.2	48
		240	140.8	47	171.2	47	163.3	47	182.9	48

Table 6: Maximum Stress Amplitude and Fatigue Life of pressure Vessels with Various Heads for Different hold periods.

Sl No	Rate of Change of Temp. °C/min.	Hold Period min.	Hemishperical		Elliptical		Torispherical		Toriconical	
			S_a	$N_f x10^5$ cycles	S_a	$N_f x10^5$ cycles	S_a	$N_f x10^5$ cycles	S_a	$N_f x10^5$ cycles
1	1.0	0	107.4	3.2235	131.9	1.5848	132.8	1.3894	153.5	0.8566
		60	109.8	2.9625	135.3	1.4179	137.7	1.1948	159.9	0.7408
		120	111.8	2.7690	137.9	1.2912	141.5	1.0680	164.9	0.6640
		180	113.4	2.6102	140.0	1.2096	144.6	0.9759	168.9	0.6098
		240	114.8	2.4812 (-23%)	141.8	1.1437 (-28%)	147.2	0.9077 (-34%)	172.1	0.5706 (-36%)
2	1.5	0	129.0	1.6788	155.1	0.8240	145.4	1.0391	153.0	0.8576
		60	133.4	1.5000	161.2	0.7070	152.31	0.8803	163.9	0.6747
		120	136.5	1.3947	165.5	0.6450	157.0	0.7862	172.1	0.5696
		180	138.9	1.3228	168.7	0.6019	160.5	0.7236	178.2	0.5053
		240	140.8	1.2833 (-50%)	171.2	0.5817 (-50%)	163.3	0.6813 (-26%)	182.9	0.4641 (-14%)

Table 7: Maximum Stress Amplitude (MPa) without and with Skirt heating (Heating and Cooling for 4 hours at 1°C/min., hold period nil, temperature change 5° to 245°C.)

Sl No	Section	Hemispherical		Elliptical		Torispherical		Toriconical	
		Skirt without heating MPa	Skirt with heating MPa	Skirt without heating MPa	Skirt with heating MPa	Skirt without heating MPa	Skirt with heating MPa	Skirt without heating MPa	Skirt with heating MPa
1	Upper head	25.5	25.5	33.6	33.6	48.7	48.7	92.6	92.6
2	Cylinder	40.4	40.4	42.4	39.9	46.0	44.0	74.6	67.2
3	Lower head	40.4	25.0	70.0	30.1	61.1	43.5	106.3	85.7
4	Skirt	107.4	6.5	132.0	28.0	132.8	33.6	153.5	65.6

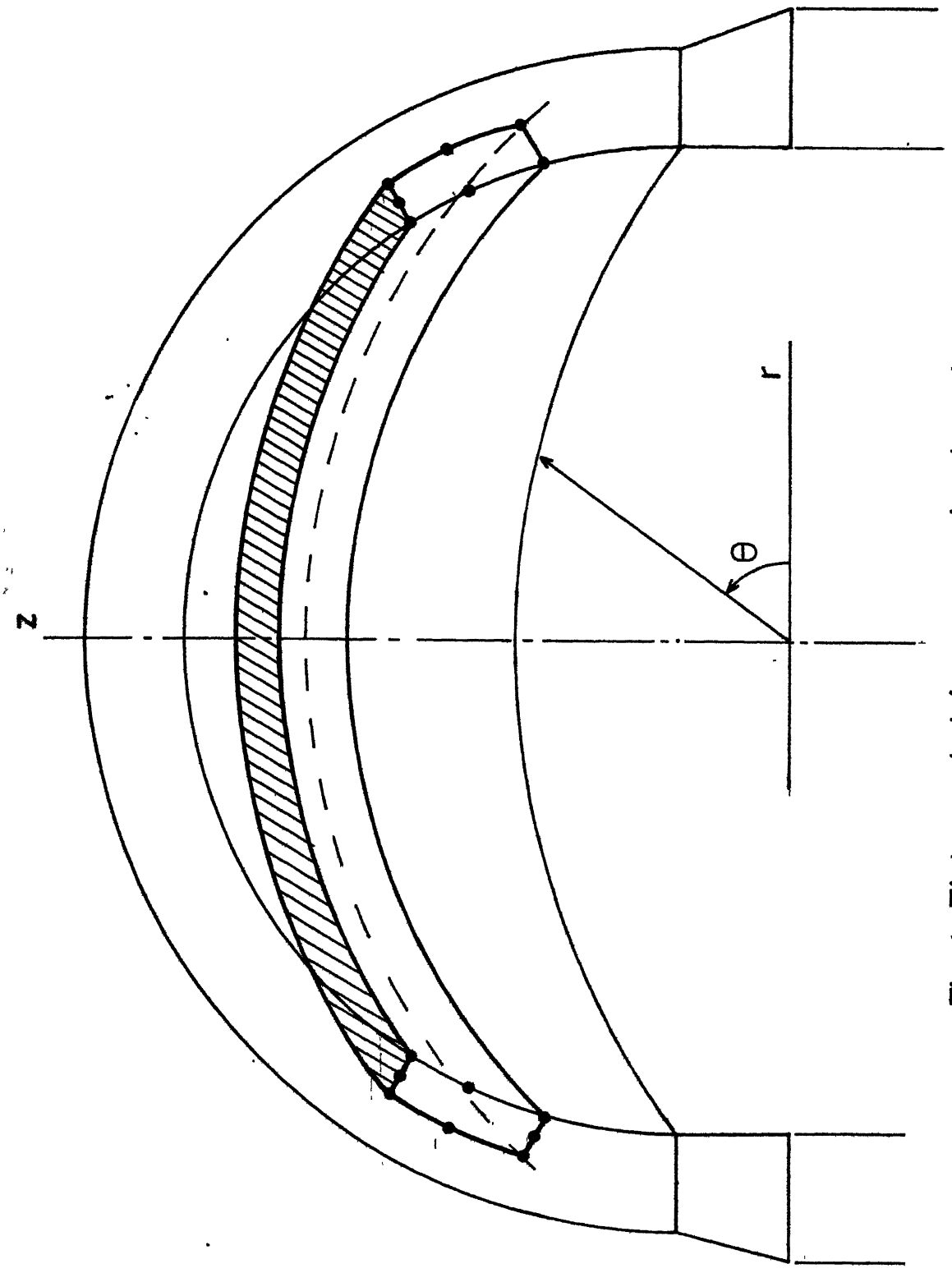

Fig. 1 Eight noded isoparametric ring element.

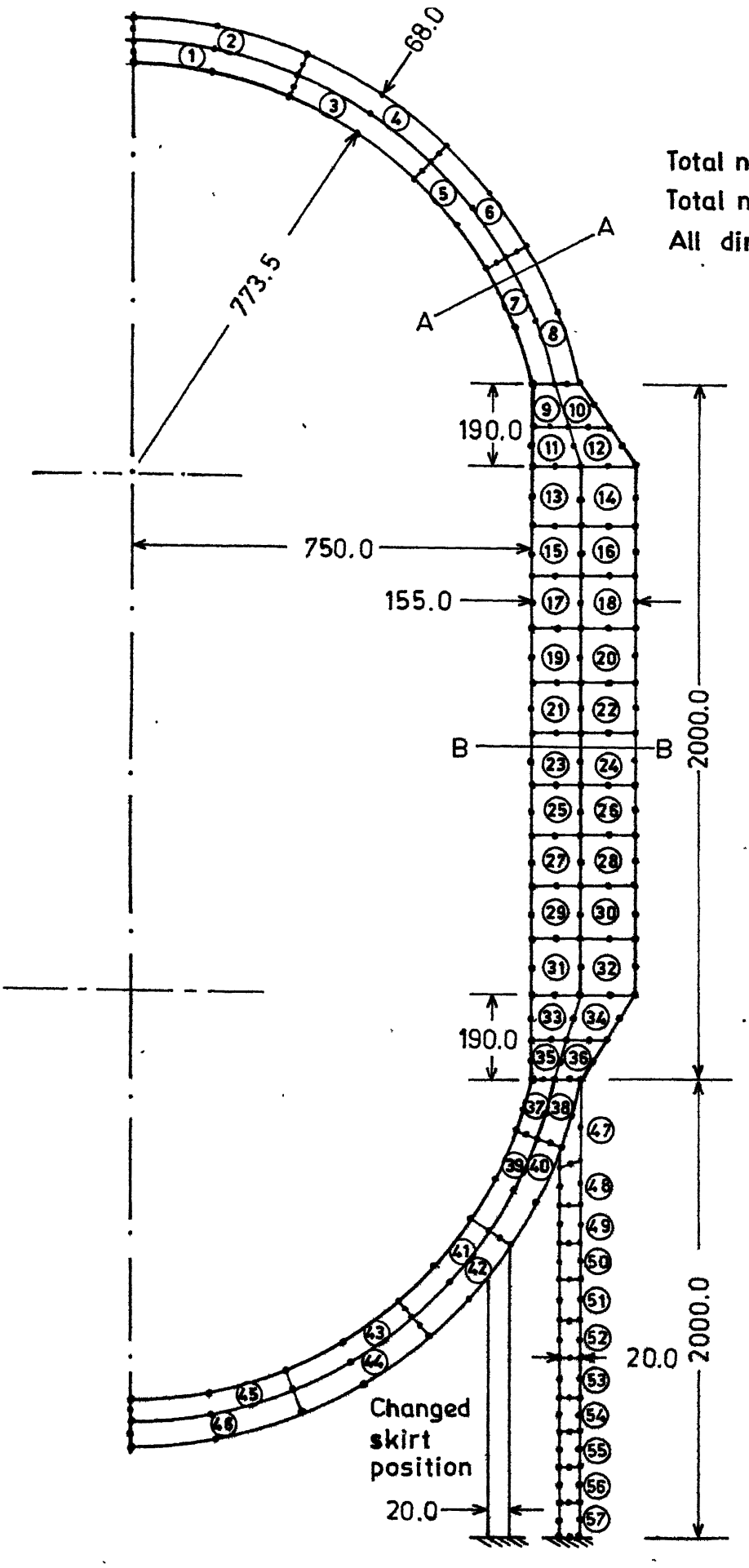

Fig. 2 Pressure vessel with hemispherical head.

Total no. of elements 57
Total no. of nodes 244
All dimensions in mm

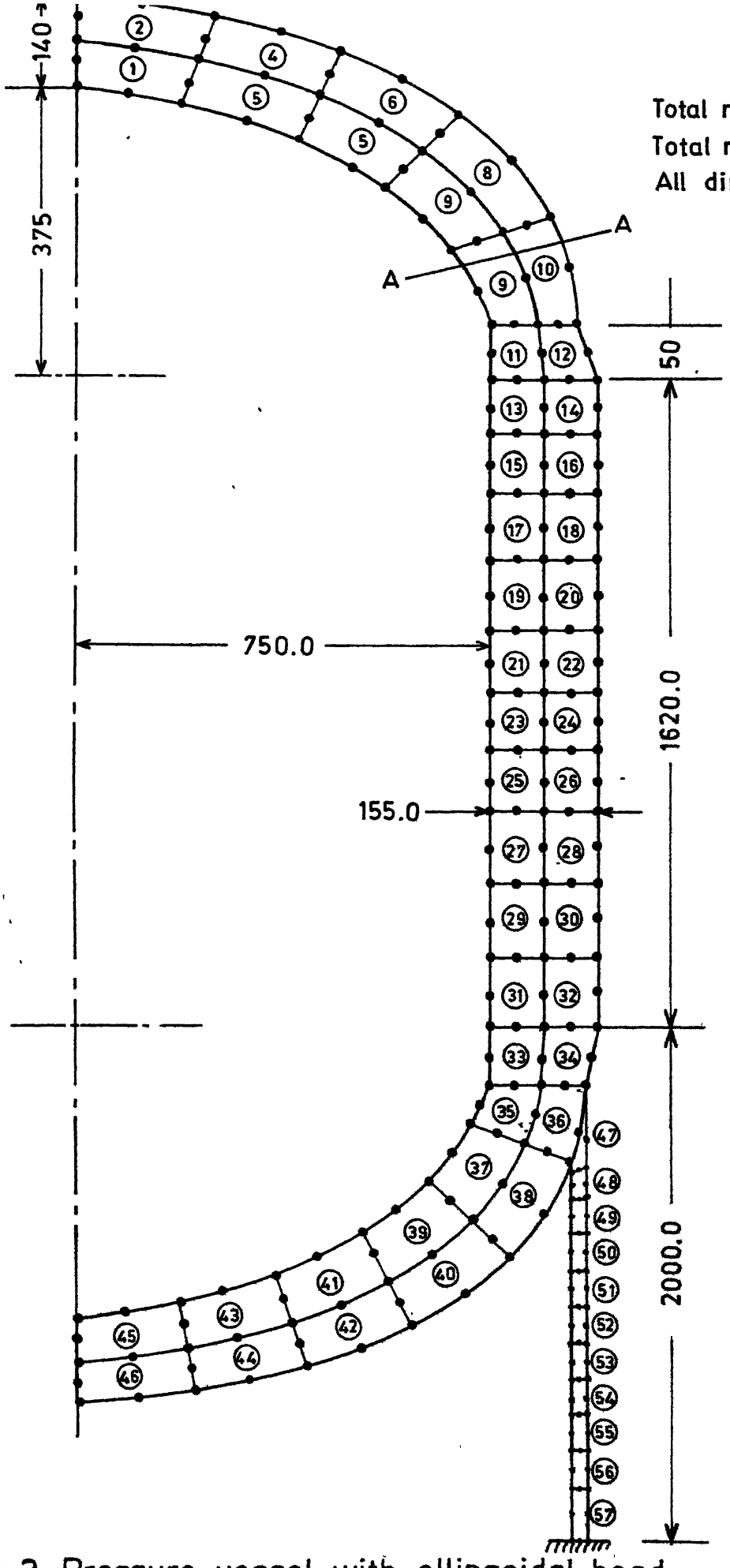

Fig. 3 Pressure vessel with ellipsoidal head.

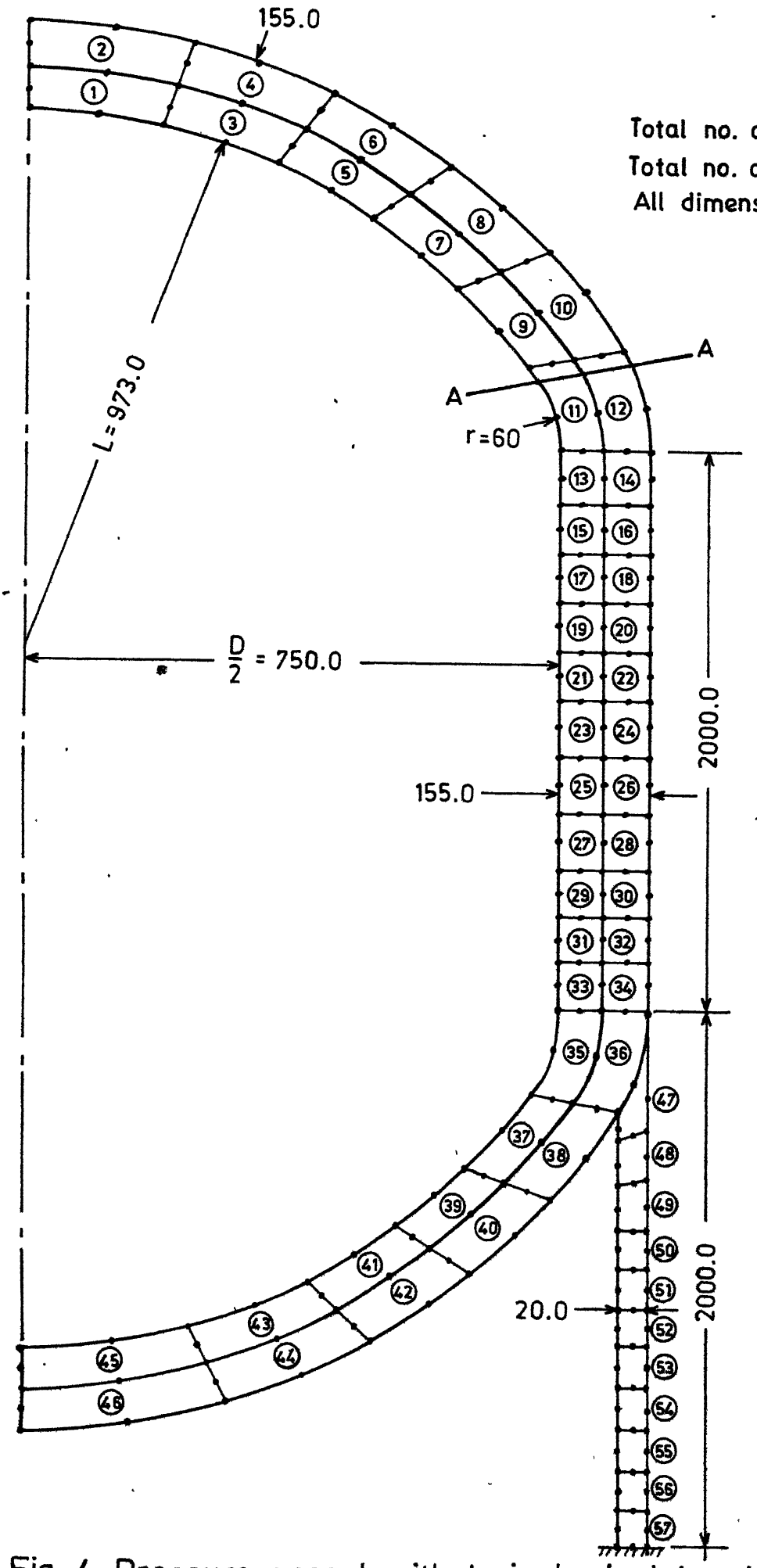

Fig. 4 Pressure vessel with torispherical head.

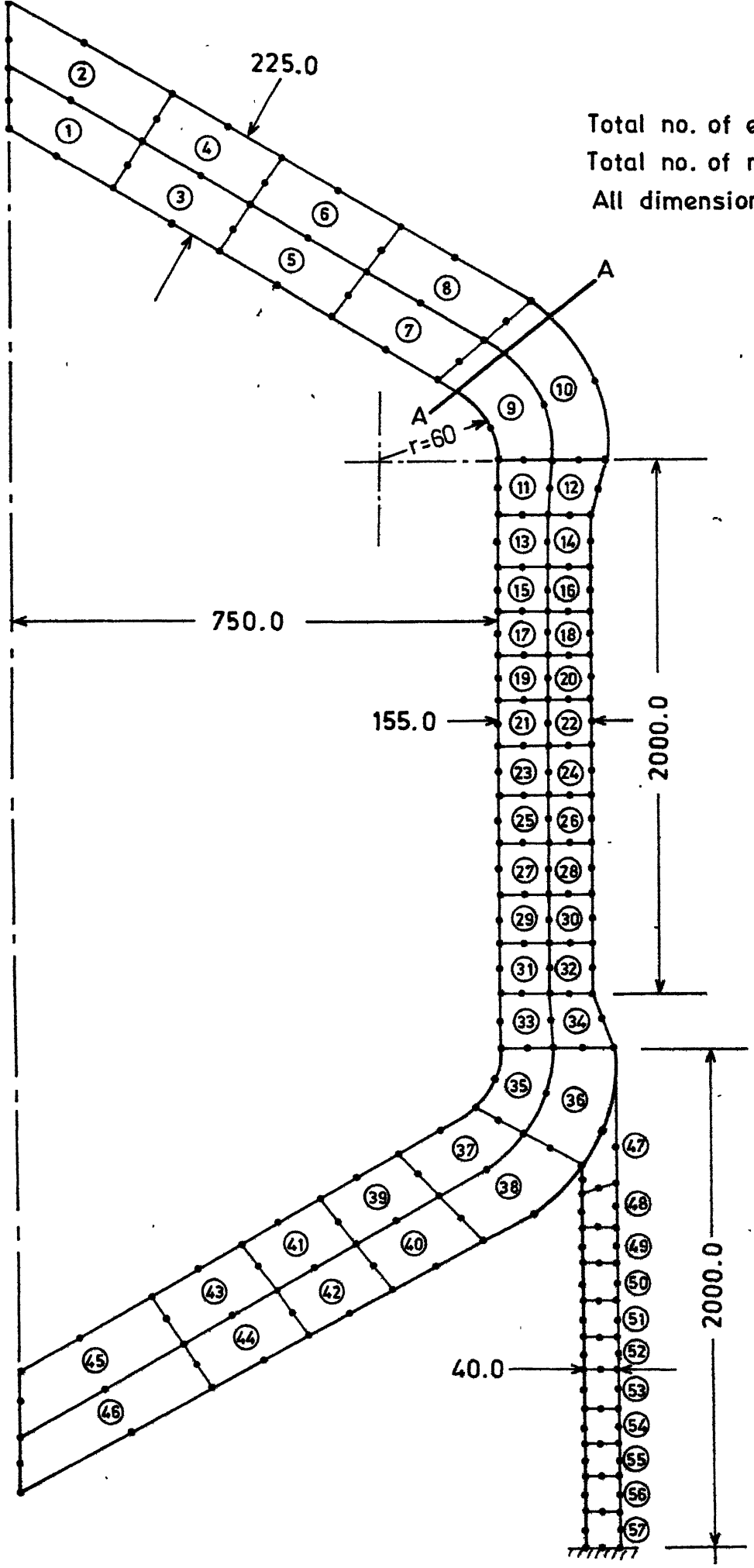

Fig. 5 Pressure vessel with toriconical head.

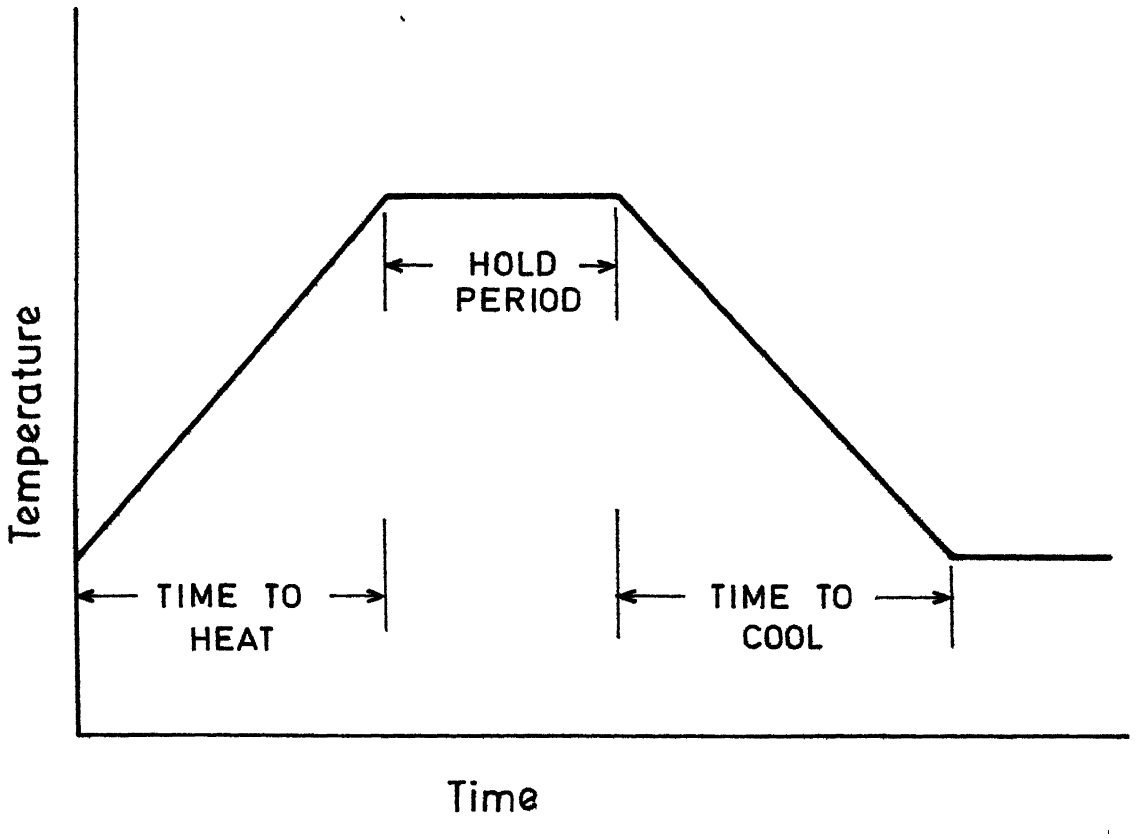

Fig. 6 Thermal cycle.

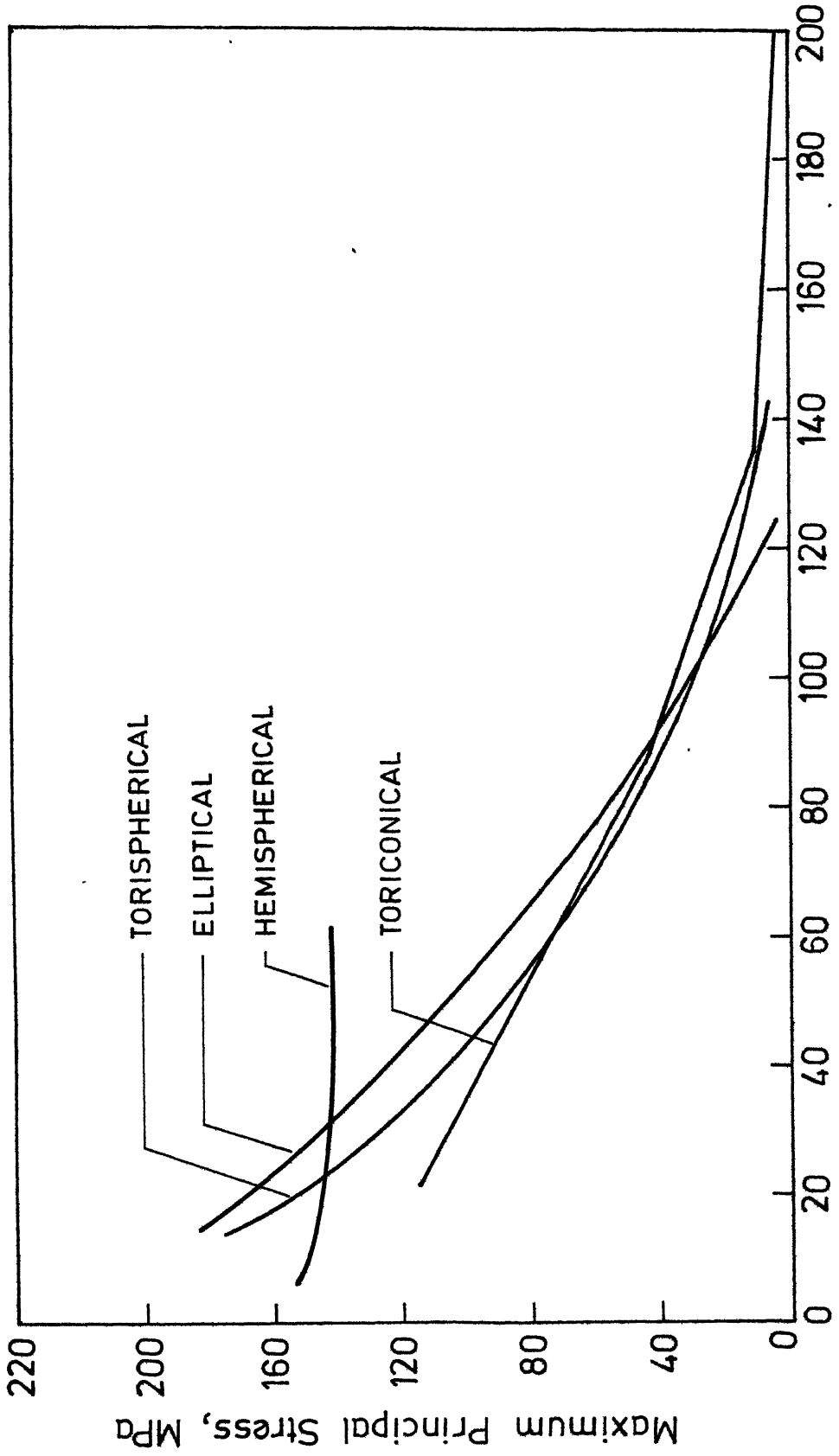

Fig. 7 Maximum principal stress across AA in upper heads due to mechanical loading.

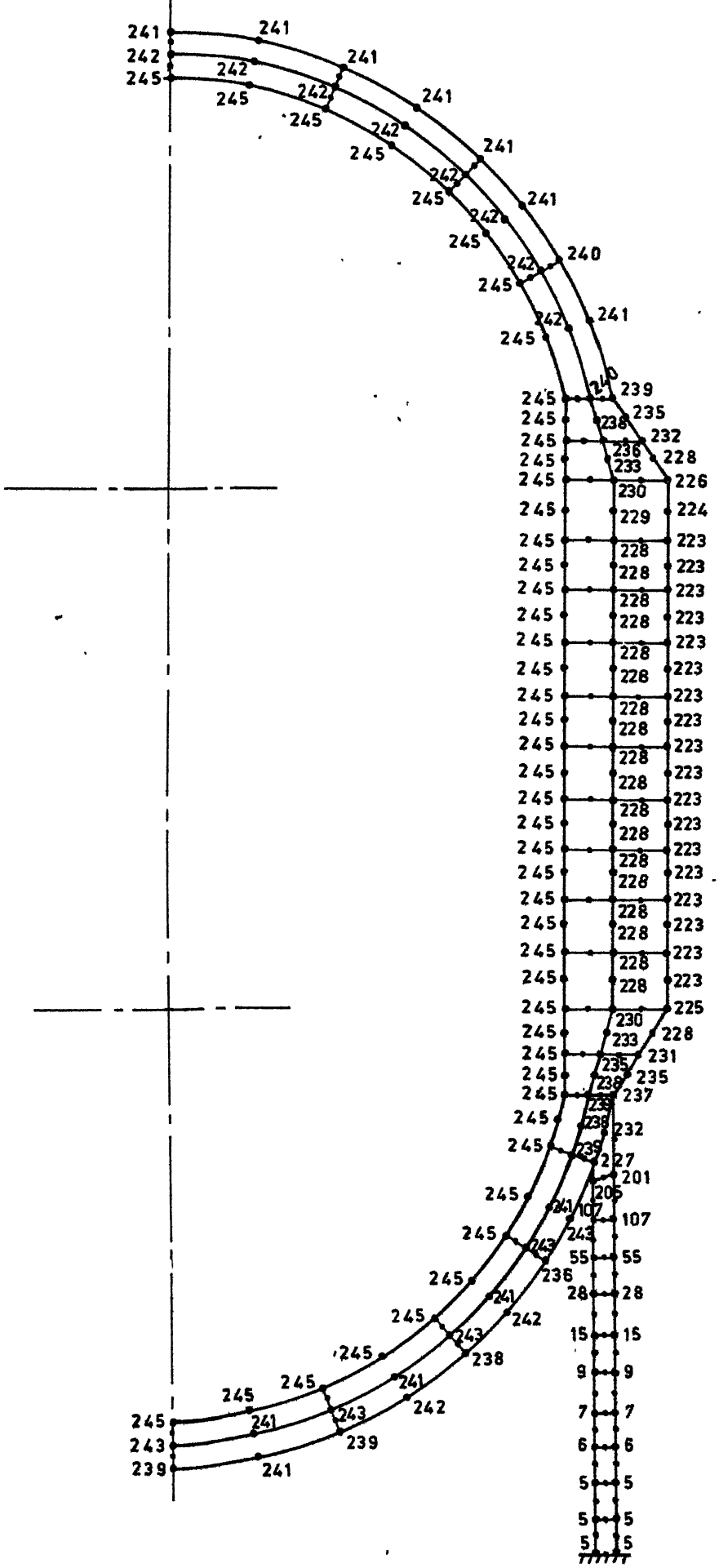

Fig. 8 Temperature distribution at the end of heating for vessel with hemispherical head.

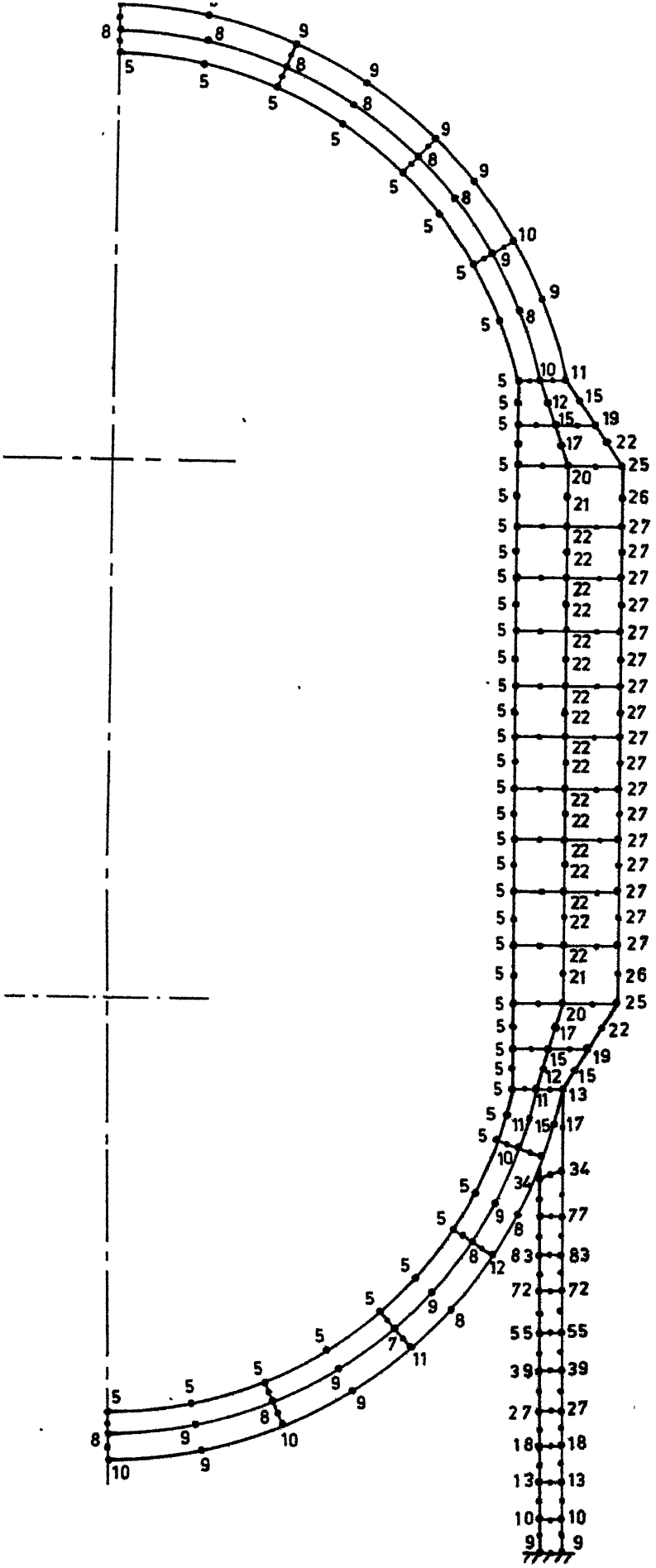

Fig. 9 Temperature distribution at the end of cooling for the vessel with hemispherical head.

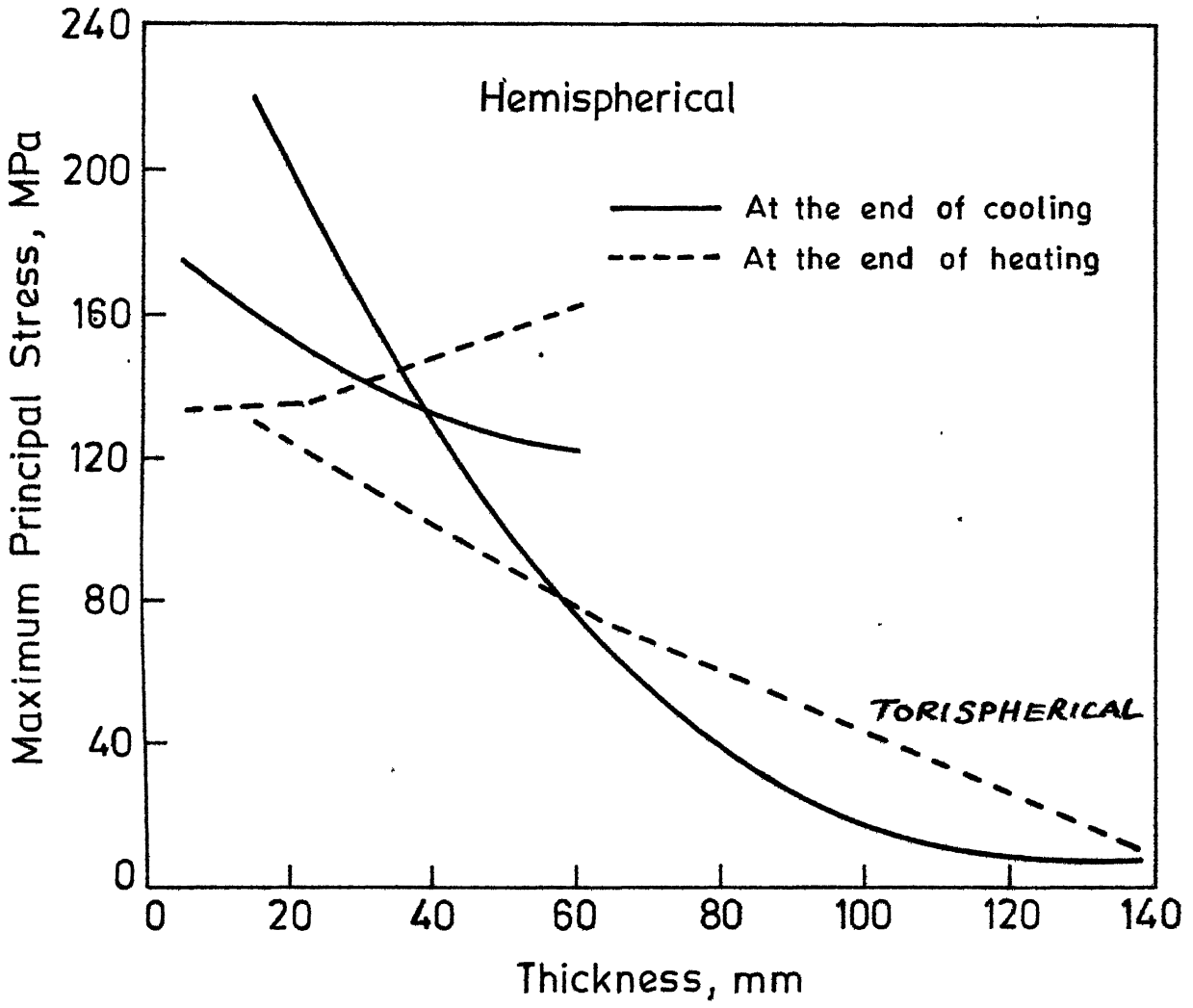

Fig. 10 Maximum principal stress across AA in the upper heads due to mechanical and thermal loading. (Typical Thermal Cycle)

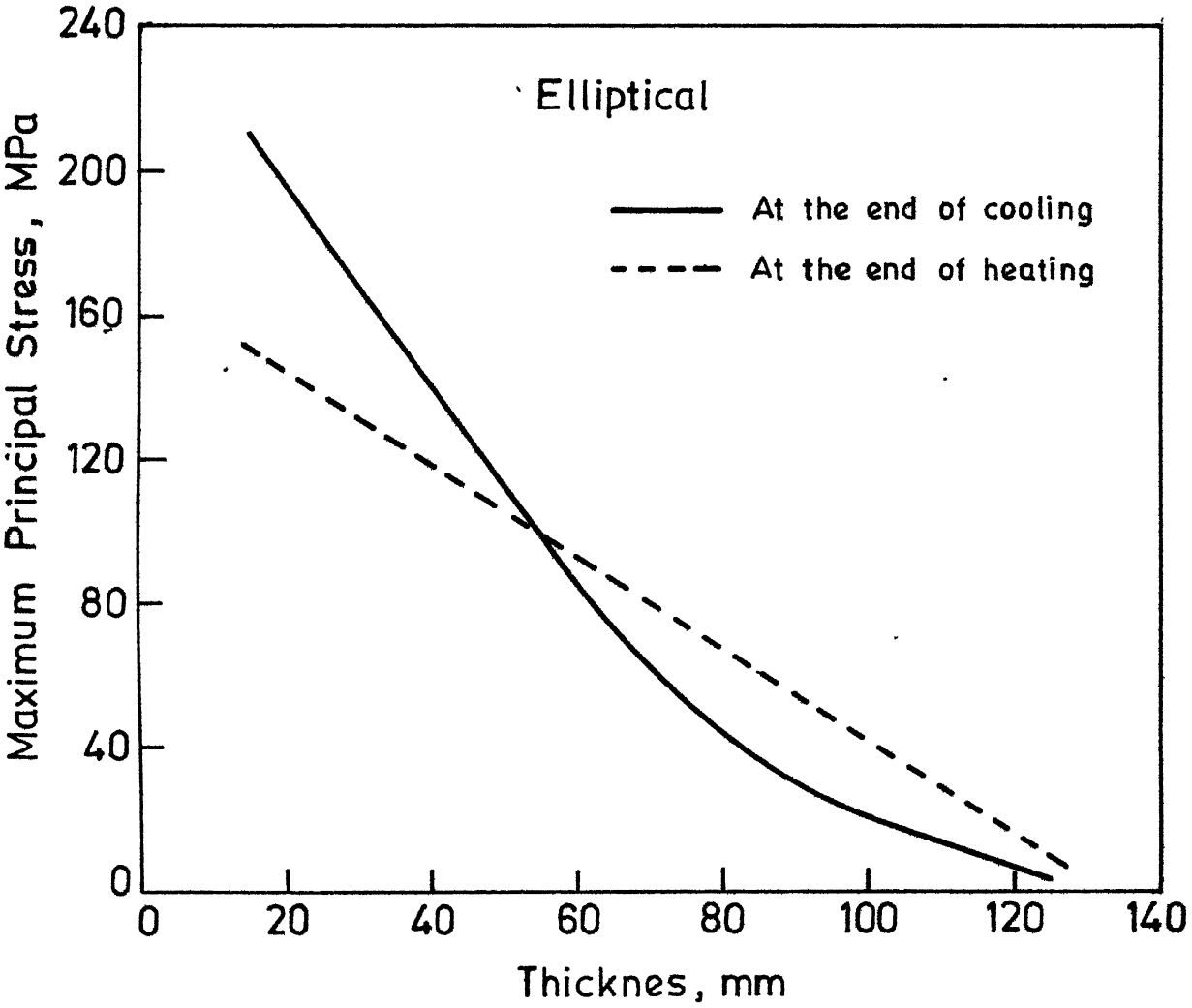

Fig. 11 Maximum Principal stress across AA in the upper heads due to mechanical and thermal loading (Typical Thermal Cycle)

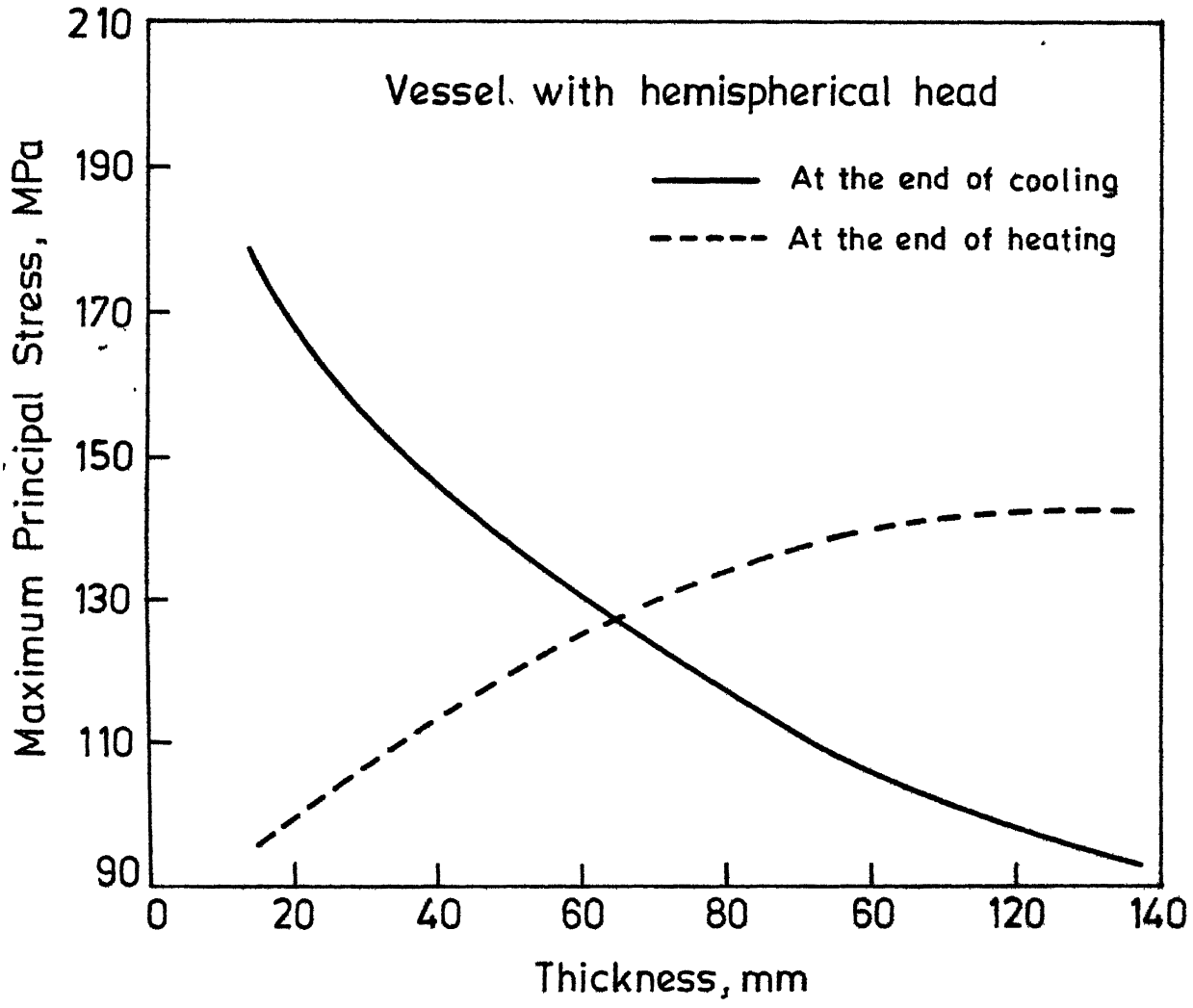

Fig. 12 Maximum principal stress across BB in the cylindrical portion due to mechanical and thermal loading (Typical Thermal Cycle)

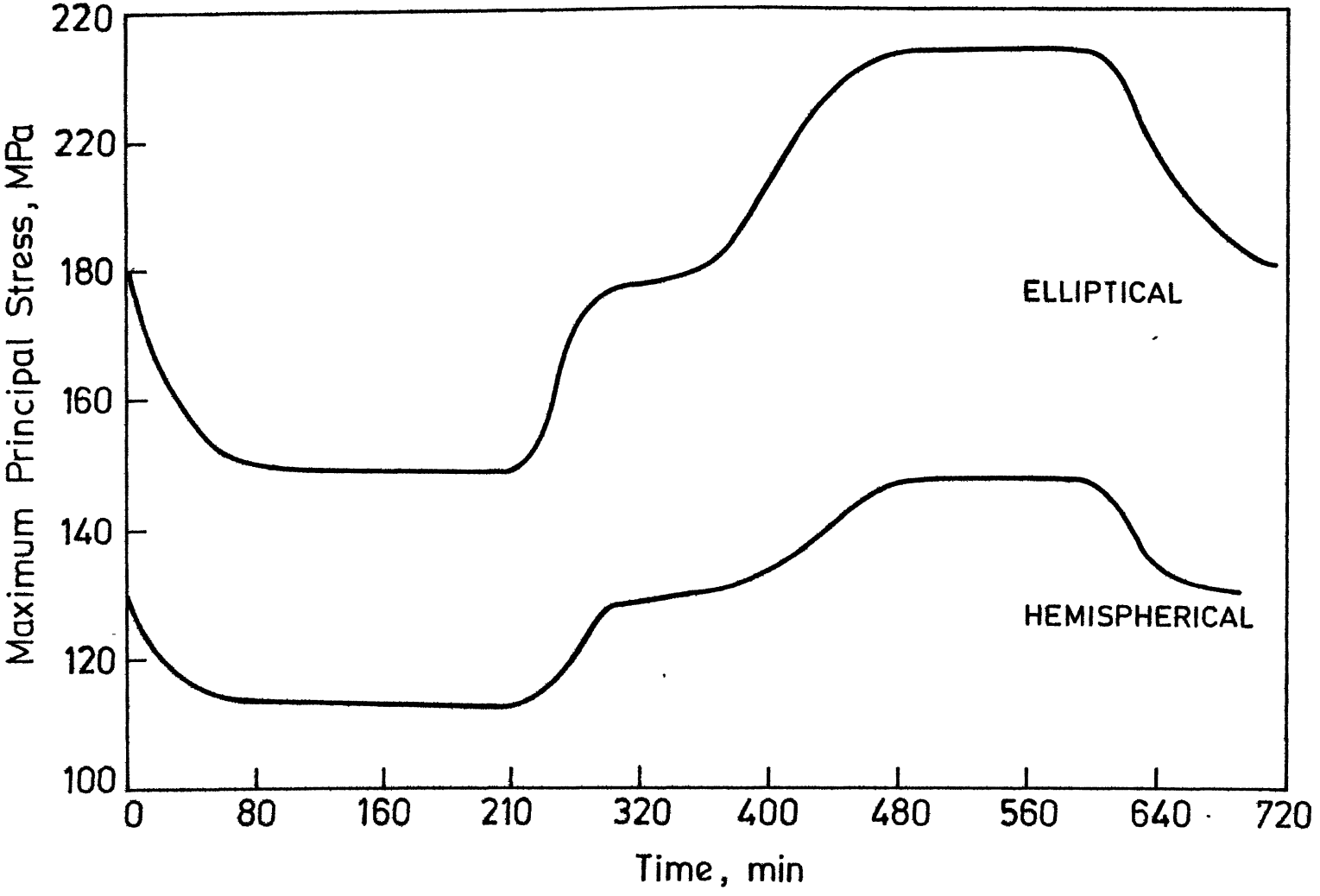

Fig. 13 Stress cycle at a point in the heads giving maximum stress amplitude.

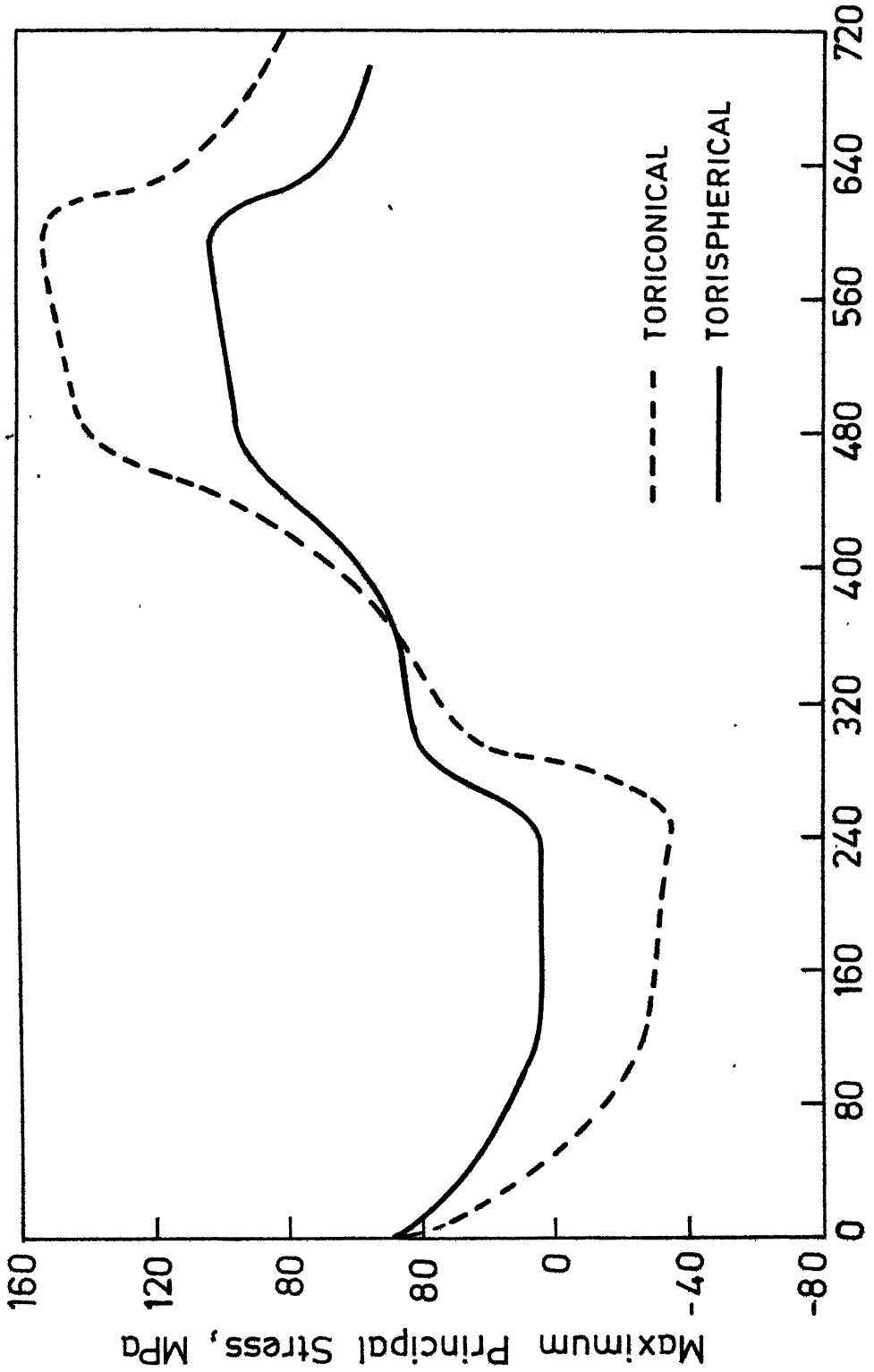

Fig. 14 Stress cycle at a point in the heads giving maximum stress amplitude.

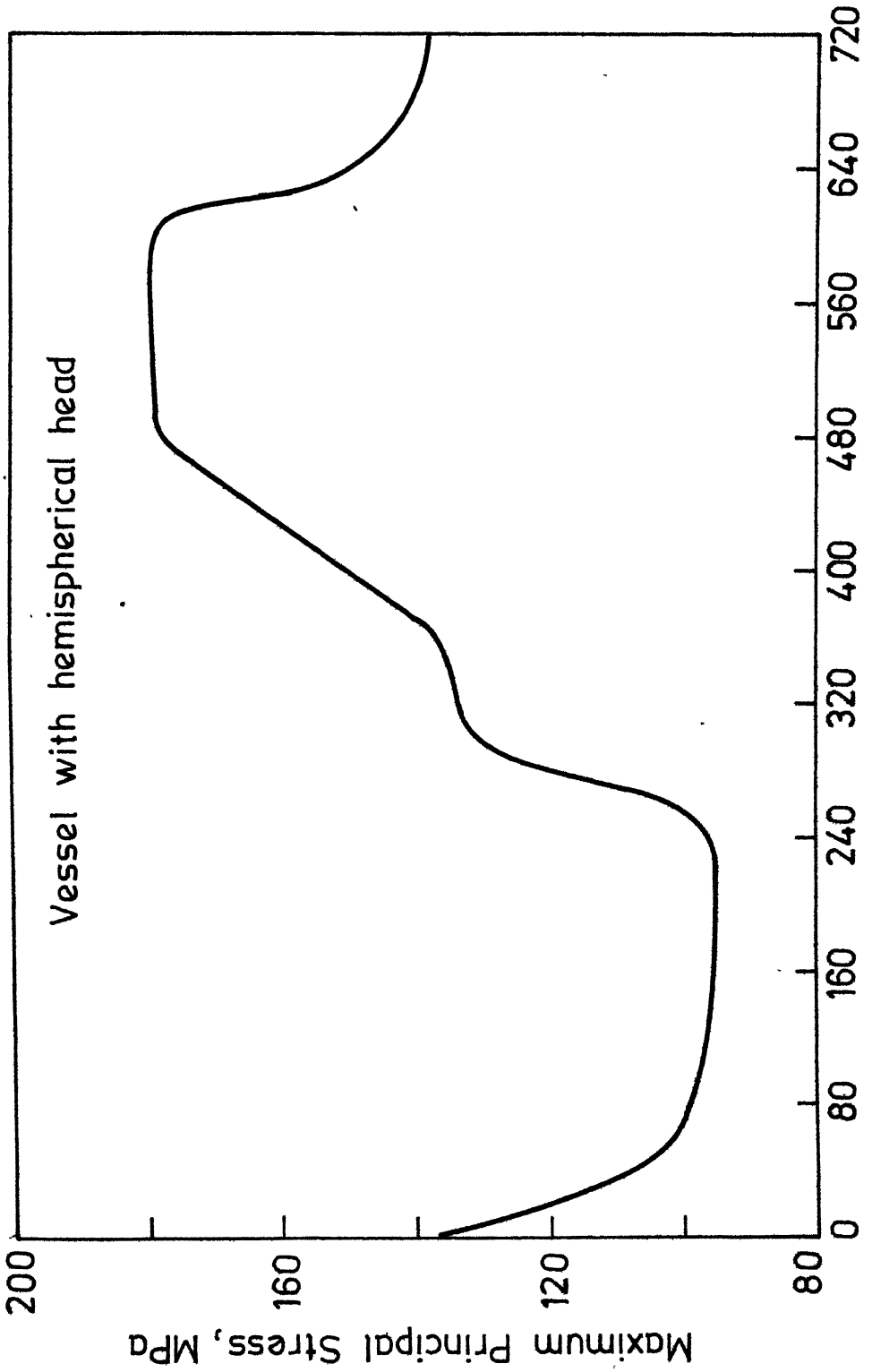

Fig. 15 Stress cycle at a point in cylindrical portion giving maximum stress amplitude.

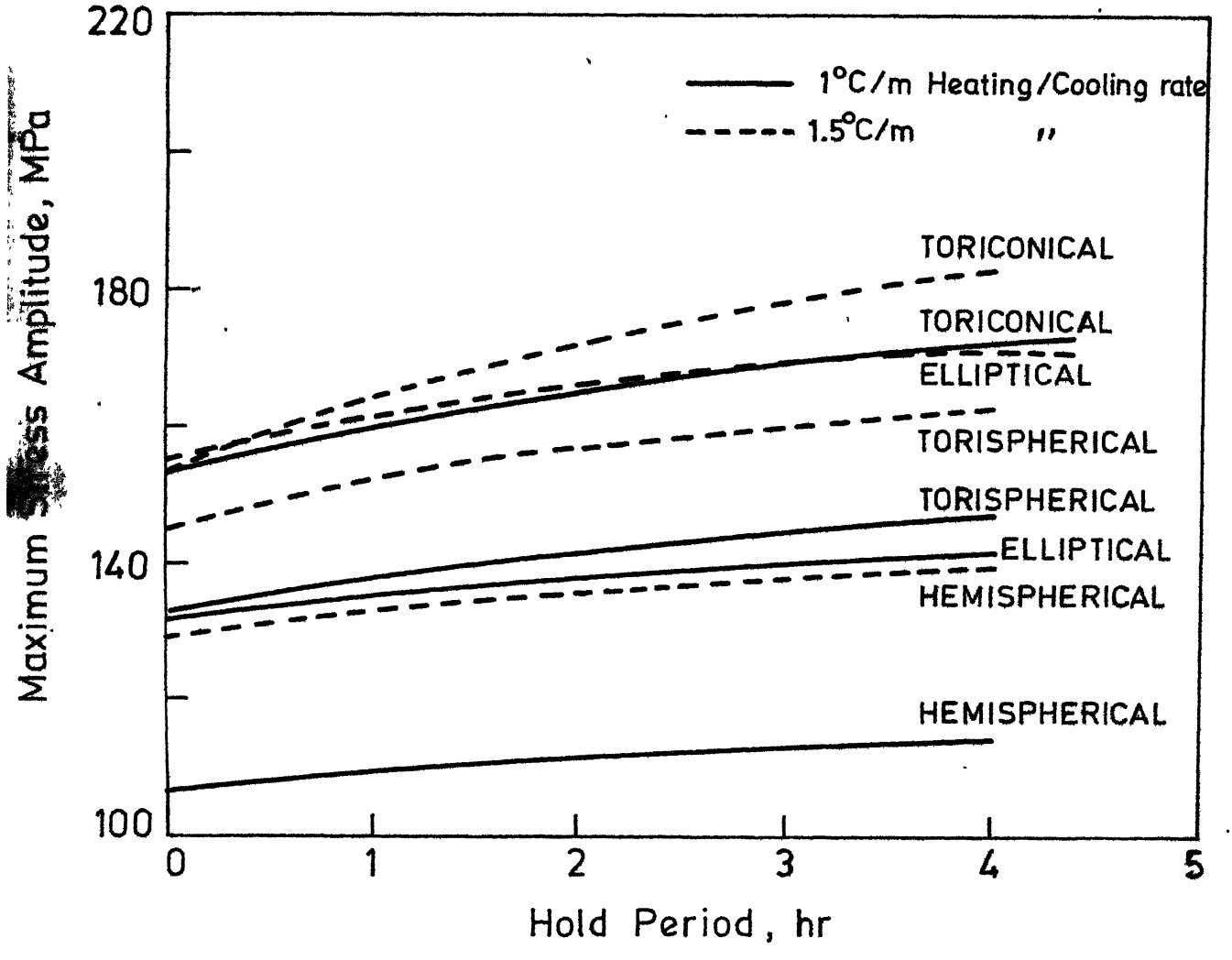

Fig. 16 Maximum stress amplitude vs hold period

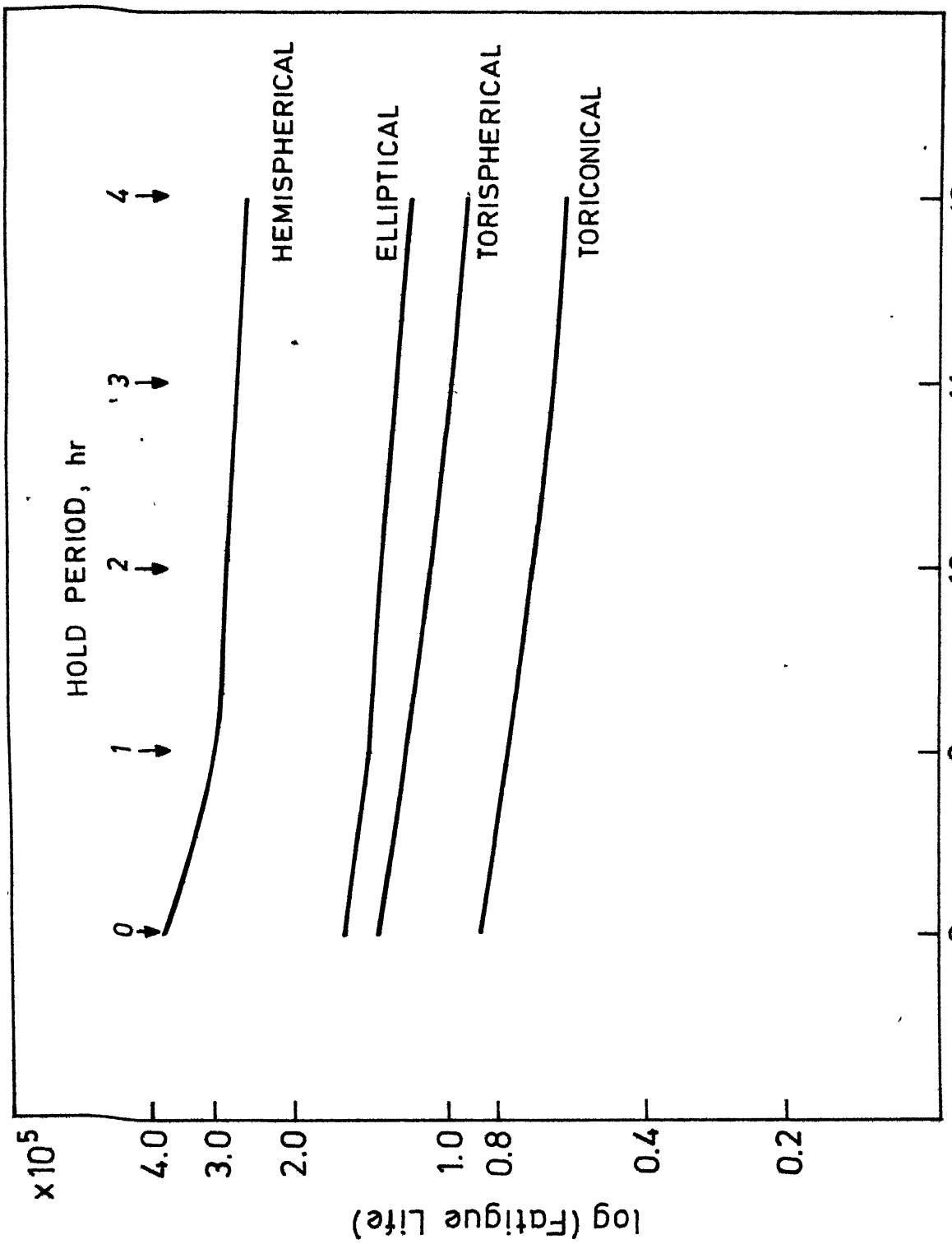

Fig. 17 Fatigue life vs cycle time.

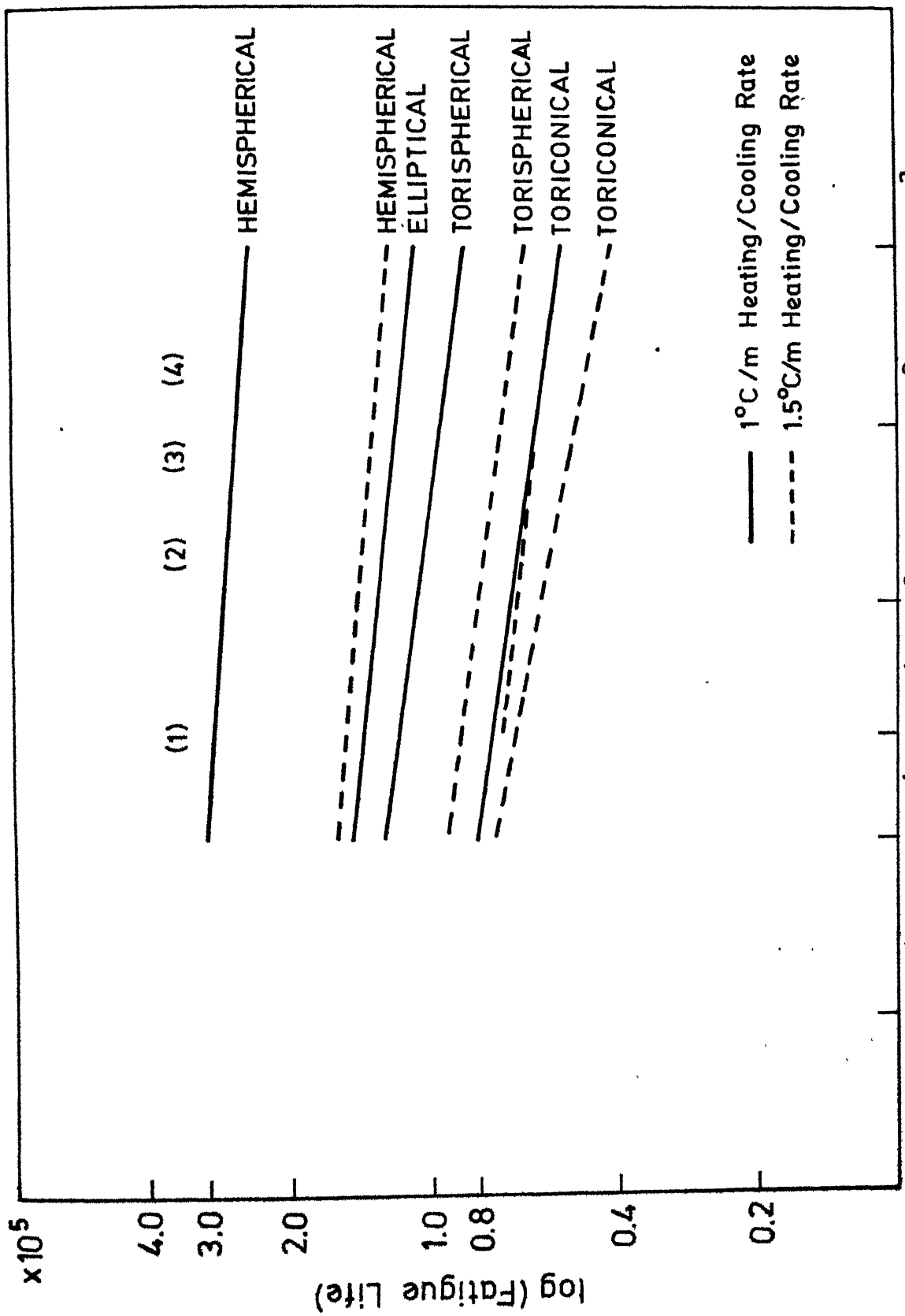

Fig. 18 Fatigue life vs hold period.

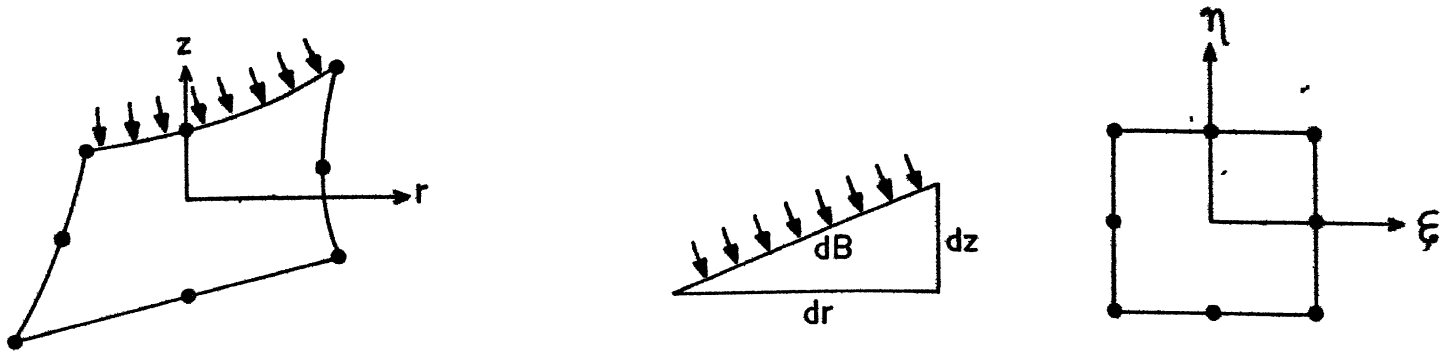

Fig. 19 Consistant surface load along an edge of an element.